

**CONTROL AUTHORITY ASSESSMENT
in
AIRCRAFT CONCEPTUAL DESIGN**

by

Jacob Kay

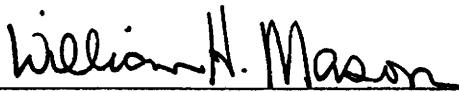
Thesis submitted to the Faculty of the
Virginia Polytechnic Institute and State University
in partial fulfillment of the requirements for the degree of

MASTER OF SCIENCE

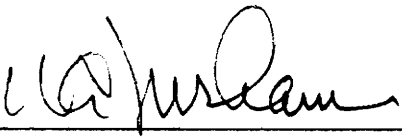
in

Aerospace Engineering

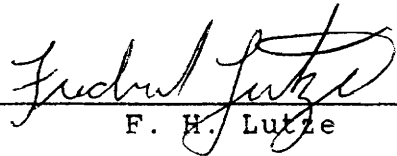
Approved:



W. H. Mason, Chairman



W. C. Durham



F. H. Lutze

December, 1992

Blacksburg, Virginia

LD
5655

V855

1992

K39

C.2

**CONTROL AUTHORITY ASSESSMENT
in
AIRCRAFT CONCEPTUAL DESIGN**

by

Jacob Kay

Committee Chairman: W. H. Mason
Aerospace Engineering

(ABSTRACT)

All aircraft must meet controllability requirements to be certified for commercial use or adopted by the military. Aircraft maneuverability is often limited by control authority. Thus, it is essential for designers to evaluate a candidate concept's control authority early in the conceptual design phase. In this thesis, a methodology for rapid control power evaluation of preliminary design configurations against requirements at the key flight conditions is established.

First, a collection of critical flight conditions to be considered using this methodology is identified. To examine a variety of aircraft configurations and accelerate the process of estimating stability and control derivatives, a FORTRAN program using the Vortex-Lattice Method was written to estimate subsonic, low angle-of-attack aerodynamics. Then, a spreadsheet processes the aerodynamic data to check whether the design configuration possesses adequate control power to satisfy the requirements of the critical flight conditions.

Acknowledgements

The author wishes to thank Dr. William H. Mason for his invaluable guidance and untiring encouragement. His extensive knowledge in airplane design is vital to this project. Recognition must also go to Drs. Durham and Lutze for serving on my committee and participating in stimulating discussions.

Support for this work was provided by Universities Space Research Association, Advanced Design Program.

Table of Contents

1.	Introduction	1
2.	Critical Flight Conditions & Maneuvers:	
	Discussion of Requirements	4
2.1	Takeoff & Landing Rotation	4
2.2	1-G Trim	6
2.3	Maneuvering Flight	7
2.4	Short Period & CAP Requirements	8
2.5	Pitch Due to Velocity Axis Roll	11
2.6	Steady Sideslip	12
2.7	Engine-Out Trim	13
2.8	Time-to-Bank	14
2.9	Rolling Pullout	18
2.10	Coordinated Roll about Velocity Axis	19
2.11	High Angle-of-Attack Departure	20
3.	Discussion of Overall Assessment Methodology	23
3.1	Flight Condition Variables	26
3.2	Stability and Control Derivatives	33
3.3	Control Power Evaluation for Requirements	41
4.	Vortex-Lattice Method	42
4.1	Code Implementation: Concept and Limitations	42
4.2	Comparison with DATCOM Estimates	
	Wind Tunnel Data	50
4.2.1	Stability Derivatives	51

4.2.2	Control Derivatives	59
5.	Control Authority Assessment Example: The F-18	65
5.1	Takeoff & Landing Rotations	65
5.2	1-G Trim	66
5.3	Maneuver Flight (Pull-up)	68
5.4	Short Period & CAP	68
5.5	Pitch Due to Velocity Axis Roll	68
5.6	Steady Sideslip	70
5.7	Engine-out Trim	70
5.8	Time-to-Bank	72
5.9	Rolling Pullout & Coordinated Roll	72
5.10	Overall Assessment	72
6.	Conclusions	74
6.1	Future Work	74
	References	76
	Appendix	
A.	Program & Spreadsheet Documentation	
A1.	Program VLM	
A2.	Spreadsheet to Check Control Authority Requirements	
A3.	Program FLTCOND	
A4.	Programs TRIM1 & TRIM2	
B.	Literature Search: Control Power Requirements	
	Vita	

List of Figures

1.	MIL-STD-1797 Short Period Dynamics Requirements	9
2.	Control Authority Assessment Methodology	24
3.	Sample Input Spreadsheet for program FLTCOND	31
4.	VLM Coordinate System	34
5.	F-18 Longitudinal Planform Representation in VLM	35
6.	Elements of Input File to VLM Program	36
7.	F-18 Lateral Profile Representation in VLM	38
8.	Sample VLM Stability & Control Derivative Output	40
9.	Vortex Rings & Control Points of VLM Implementation	44
10.	Prandtl-Glauert Correction Rule Used in VLM To Account for Compressibility	44
11.	Surface Velocity Distribution due to Pitching Rate	46
12.	Spanwise Vortex Strength Distribution for Asymmetric Loading	46
13.	Use of Mirror Vortex System to Model Ground Effect	48

14.	Vortex Rings and Corner Points of F-18 Longitudinal Planform	49
15.	Vortex Rings and Corner Points of F-18 Lateral Profile	49
16.	Angle-of-Attack Derivatives & Static Margin	52
17.	Pitch Rate Derivatives	53
18.	Sideslip Derivatives	55
19.	Yaw Rate Derivatives	56
20.	Roll Rate Derivative	57
21.	Elevator (Horizontal Tail) Effectiveness	60
22.	Inboard Trailing Edge Flap Effectiveness	61
23.	Aileron Effectiveness	63
24.	Rudder Effectiveness (One-Rudder Deflection)	64
25.	Estimated Maximum Stability Axis Roll Rate of F-18 Limited by Elevator Power, @ SL, Mach 0.6	69

List of Tables

1.	Time-to-Bank Requirements from MIL-STD-1797	
	a. General Roll Performance for Class IV Airplanes	15
	b. Air-to-Air Combat Roll Performance Requirements	15
	c. Air-to-Air Combat Roll Performance Requirements	16
	d. Ground Attack Roll Performance Requirements	16
2.	Sample Output File of program FLTCOND	32
3.	Reliability of Stability Derivative Predictions Compared to Wind tunnel Data	58
4.	1-G Trim Control Authority Assessment	67
5.	Maneuver Flight (Pull-up) Control Authority Assessment	67
6.	Short Period & Control Anticipation Parameter (CAP) Assessment	69
7.	Engine-out Trim Assessment at Mach 0.2 at S.L.	71
8.	Time-to-Bank Performance at SL ($I_x = 26,000$ slug ft ²)	73
9.	Rolling Pullout & Coordinated Roll Assessment at S.L., Mach 0.6	73

List of Symbols

<u>Symbol</u>	<u>Definition</u>	<u>Dimension</u>
b	Wing/planform Span	ft
CAP	Control Anticipation Parameter	rad/(g s ²)
c, \bar{c}	Reference chord	ft
g	Gravitational Acceleration: 32.2	ft/s ²
$I_{x,y,z}$	Inertia about x-, y-, z- Axis	slug ft ²
i_T	Vertical Thrust Incident Angle w/ Fuselage Reference Line (+ for jet exhaust downward)	rad
L_p	$(dl/dp)/I_x$	/s
L_r	$(dl/dr)/I_x$	/s
$L_{\delta R}$	$(dl/d\delta R)/I_x$	/s ²
$L_{\delta A}$	$(dl/d\delta a)/I_x$	/s ²
M	Mach Number	
m	Airplane Mass	slug
N_p	$(dn/dp)/I_z$	/s
N_r	$(dn/dr)/I_z$	/s
$N_{\delta R}$	$(dn/d\delta R)/I_z$	/s ²
$N_{\delta A}$	$(dn/d\delta a)/I_z$	/s ²
$n_o(-), n_o(+)$	Minimum & Maximum Operational Load Factor	g
n_z	Normal Load Factor	g
p	Velocity Axis Roll Rate	rad/s

q	Pitch Rate	rad/s
\bar{q}	Dynamic Pressure	lbf/ft ²
r	Velocity Axis yaw Rate	rad/s
S	Wing Reference Area	ft ²
T	Thrust	lbf
T	Aileron Servo Time Constant	s
V	Speed	ft/s
W	Airplane Weight	lbf
x, z	Horizontal & Vertical Distance between C.G. and Main Gear Axle (+ for axle behind and below CG)	ft
x_T, z_T	Horizontal & Vertical Distance between Engine Nozzle and C.G. (+ for nozzle Behind and above C.G.)	ft
α	Angle of Attack	rad
β	Sideslip Angle	rad
β	Prandtl Glauer Correction Factor	
ΔT	Thrust Difference	lbf
$\delta E, \delta F, \delta A, \delta R$	Elevator, Flap, Aileron, Rudder Deflection	rad
ϕ	Bank Angle	rad, deg
γ	Climb Angle	rad, deg
μ	Rolling Friction Coefficient	
ω_{nsp}	Short Period Natural Frequency	/s
ρ	Air Density	slug/ft ³
$\theta_{tipback}$	Tipback angle (Arctan(z/x))	rad
ξ	Damping Ratio	

Non-dimensional Stability & Control Derivative System:

C_{xy} Variation of x with non-dimensionalized y

Subscripts:

α , alpha	Angle of Attack
$\dot{\alpha}$, alpha-dot	Angle of Attack Rate
β , beta	Sideslip Angle
δA , delta A	Aileron Deflection
δE , delta E	Elevator Deflection
δF , delta F	Flap Deflection
δR , delta R	Rudder Deflection
D	Drag
L	Lift
l	Rolling Moment
m	Pitching Moment (about CG)
n	Yawing Moment
p	Roll Rate
q	Pitch Rate
r	Yaw Rate
T	Thrust
y	Sideforce
C_{L0} , C_{m0}	C_L & C_m at 0-deg AOA

Symbols for VLM Program

CL0	C_L at 0-deg AOA with x-axis as the fuselage reference line.
CM0	C_m at 0-deg AOA with x-axis as the fuselage reference line.
CL-alpha	$C_{L\alpha}$ (/rad)
Cm/CL	dC_m/dC_L
CL-q	C_{Lq} (/rad) $\frac{\partial C_L}{\partial(\frac{qC}{2V})}$
CM-q	C_{mq} (/rad) $\frac{\partial C_m}{\partial(\frac{qC}{2V})}$
DCL(i,j)	$dC_L/d\delta$ control surface (i = section #, j = 1 for LE flap; j = 2 for TE flap) with symmetric deflection for control surfaces modelled in the longitudinal case
DCM(i,j)	$dC_m/d\delta$ control surface (i = section #, j = 1 for LE flap; j = 2 for TE flap) with symmetric deflection
Cl-p	C_{lp} (/rad) $\frac{\partial C_l}{\partial(\frac{pb}{2V})}$
Cn-p	C_{np} (/rad) $\frac{\partial C_n}{\partial(\frac{pb}{2V})}$
DCroll(i,j)	$dC_l/d\delta$ control surface (i = section #, j = 1 for LE flap; j = 2 for TE flap) with antisymmetric deflection for control surfaces modelled in the longitudinal case
DCyaw(i,j)	$dC_n/d\delta$ control surface (i = section #, j = 1 for LE flap; j = 2 for TE flap) with antisymmetric deflection for control surfaces modelled in the longitudinal case
Cy-beta	$C_{y\beta}$ (/rad)

Cn-beta	$C_{n\beta}$ (/rad)	
Cl-beta	$C_{l\beta}$ (/rad)	
Cy-r	C_{yr} (/rad)	$\frac{\partial C_y}{\partial(\frac{rb}{2V})}$
Cn-r	C_{nr} (/rad)	$\frac{\partial C_n}{\partial(\frac{rb}{2V})}$
Cl-r	C_{lr} (/rad)	$\frac{\partial C_l}{\partial(\frac{rb}{2V})}$
DCy(i,j)	dC _y /dδcontrol surface (i = section #, j = 1 for LE flap; j = 2 for TE flap) for control surfaces modelled in the lateral/directional case	
DCn(i,j)	dC _n /dδcontrol surface (i = section #, j = 1 for LE flap; j = 2 for TE flap) for control surfaces modelled in the lateral/directional case	
DCl(i,j)	dC _l /dδcontrol surface (i = section #, j = 1 for LE flap; j = 2 for TE flap) for control surfaces modelled in the lateral/directional case	

1. Introduction

Conventional aircraft control authority is determined by the size and placement of control surfaces. With increasing demand for agility, and use of advanced flight control systems coupled with relaxed static stability, consideration of control power has become an important issue in aircraft design. However, excessive control authority can translate into increased weight and drag. The designers' goal when sizing and placing control surfaces is to provide sufficient control power to meet the requirements of prescribed maneuvers, military specifications (MIL-STD-1797), and certification guidelines (FAR Parts 23 & 25).

Traditionally, low airspeed and adverse atmospheric conditions such as gusts place the greatest demand on control authority of most aircraft. Agile maneuvers accomplished by frequent excursions into high angle-of-attack regimes and high roll performance can result in adverse coupling effects. Therefore, it is important to assess the control power of a proposed design concept against the performance requirements early in the conceptual design stage.

The primary objective of this work is to establish a methodology that can be easily used by designers using a PC to rapidly assess the control power of preliminary design concepts against their requirements. First, requirements of maneuvers and flight conditions that are known to place

critical demands on control power are identified. The related parameters and the governing equations are listed for each maneuver requirement. A design's flight condition variables such as altitude, airspeed, CG location, load factor, etc. will vary widely. A FORTRAN program with spreadsheet input was created to identify the critical combinations of these variables for each requirement evaluation for a particular design concepts.

To evaluate the design for control power, stability and control derivatives must be estimated from the geometry of the design configuration. Traditionally, the US Air Force Stability and Control DATCOM (Ref. 1) has been the primary means of estimating the aerodynamic properties prior to tunnel tests in the conceptual design stage. However, this approach is limited to more conventional configurations and can be very time consuming. Therefore, a program using the subsonic vortex-lattice method was written to expedite this process for the subsonic (up to around Mach 0.6) and low angle-of-attack flight regimes. Its effectiveness demonstrates the feasibility of applying computational methods as design tools, and it will serve as the foundation for future development. Once the aerodynamic characteristics are estimated, these characteristics can be used in the appropriate equations to determine if the design configuration possesses sufficient control power using a series of simple spreadsheets. One

should note that the control authority evaluation process does not address high angle-of-attack stability and control requirements because of the difficulty in estimating high AOA aerodynamic characteristics.

To apply this methodology, the following information regarding the candidate concept is needed:

1. Layout of the major components and control surfaces
2. Mass properties: CG travel, weight and inertia variations (can be estimated using Ref. 2 & 3).
3. Extreme performance objectives: Maximum Mach vs. altitude; Maximum load factor and maximum and minimum thrust limits

The FORTRAN programs used in this study were written in FORTRAN 77 and were compiled on Microsoft Fortran for IBM compatible personal computers and can be modified to run on other computer systems. Lotus-123 was used to create the worksheet on which the control authority is tested against the requirements.

2. Critical Flight Conditions and Maneuvers: Discussion of Requirements

The goal of this section is to identify maneuvers and flight conditions that usually require substantial control authority to achieve desirable flight characteristics. Specifications set by MIL-STD-1797 (Ref. 4) and MIL-F-8785C are the basis of the requirements. However, the scope of this study does not include any unsteady characteristics such as the rate limits of the control servos and the effects of aeroelasticity.

2.1 Takeoff & Landing Rotations

According to the section 4.2.7.3 of MIL-STD-1797, at $0.9 V_{\min}$, the aircraft must be able to obtain the pitch attitude that will result in takeoff at V_{\min} for dry, prepared runways. For conventional nose-wheeled aircraft, this scenario is most critical for maximum takeoff gross weight, or with a stores arrangement resulting in the CG being located at its most forward location. To verify compliance with this requirement, one must first determine the minimum rotation speed. This speed occurs when the aircraft first obtains enough dynamic pressure for its pitch controller to generate a net nose-up moment with the nose wheel clear of the ground (ie. providing no force contribution). Accounting for the pitching moments about the main gear axle with contributions from thrust and

drag, the following equation (based on the discussion in section 2.5.3.1 of Ref. 5) can be used to determine the nose-wheel lift-off speed:

$$V_{LO} = \left[\frac{\left(\frac{W}{S} - \frac{T}{S} \sin(i_T) \right) (x + \mu z) + \frac{T}{S} (z_T \cos(i_T) + x_T \sin(i_T))}{\frac{1}{2} \rho (\bar{C}C_m + C_L(x + \mu z))} \right]^{\frac{1}{2}} \quad (1)$$

C_L and C_m are the total aerodynamic lift and pitching moment (about the CG) coefficient of the entire aircraft in ground effect with flaps set in takeoff position and pitch controllers fully deflected for nose-up moment. The nose-wheel lift-off speed must be smaller than $0.9 V_{min}$. In addition, one must also check to determine if adequate control power exists to continue rotating to takeoff pitch attitude prior to reaching $0.9 V_{min}$. This can be accomplished by performing a simulation of the rotation process using:

$$M_{CG} = -(W - L - T \sin(i_T + \alpha)) (\sin(\theta_{tipback} - \alpha) + \mu \cos(\theta_{tipback} - \alpha) \sqrt{x^2 + z^2}) - T(z_T \cos(i_T) + x_T \sin(i_T)) + \bar{C}S\bar{q}C_m \quad (2)$$

The dynamic pressure, angle-of-attack, and aerodynamic lift and pitching moment are all time-dependent variables. The total lift and pitching moment can be approximated by:

$$C_L = C_{L_{\alpha=0}} + C_{L_\alpha} \alpha + C_{L_{\delta F}} \Delta \delta F_{Takeoff} + C_{L_{\delta E}} \Delta \delta E_{max} \quad (3)$$

$$C_m = C_{m_{\alpha=0}} + C_{m_\alpha} \alpha + C_{m_{\delta F}} \Delta \delta F_{Takeoff} + C_{m_{\delta E}} \Delta \delta E_{max} \quad (4)$$

The rotation motion can be simulated using:

$$M_{cg} = I_{y_{cg}} \ddot{\alpha} \quad (5)$$

For landing requirements, after the main gear touches down, the pitch controller must be sufficiently powerful to gently lower the nosewheel down to $0.9 V_{min}$ in the landing configuration. The design configuration must demonstrate that it can provide a net nose-up moment in the landing configuration down to the specified speed using Eq. 2. Note this requirement does not address the potentially large nose-down moment as a result of extremely high sink rate at touch down.

2.2 1-G Trim

The configuration must demonstrate that the pitch controller is capable of attaining steady 1-g level flight at all service altitudes between stall and maximum speed. Experience shows that this scenario may become important only at the limits of the flight envelope. To examine the control effectiveness, one should consider the pitch controller's

deflection to maintain level flight. The net pitching moment must equal zero, while the total aerodynamic lift is equal to the weight of the plane (ie. the plane's forces and moments must be balanced). Further, assuming the neutral point is invariant with respect to angle of attack changes, the following relations can be obtained:

$$\delta E_{trim} = \frac{C_{m_0} + \frac{\partial C_m}{\partial C_L} \left(\frac{W}{qS} - C_{L_0} \right)}{-C_{m_{\delta E}} + \frac{\partial C_m}{\partial C_L} C_{L_{\delta E}}} \quad (6)$$

$$\alpha_{trim} = \frac{-(C_{m_0} + C_{m_{\delta E}} \delta E_{trim})}{C_{L_{\alpha}} \frac{\partial C_m}{\partial C_L}} \quad (7)$$

The resulting elevator deflection angle should not exceed its range of effectiveness. These equations can also be used to determine the 1-G trim schedule. In addition, two computer programs were written based on NASA TP-2907 to determine the optimal longitudinal trim solution for aircraft with 3 lifting-surface or 2 lifting-surface + thrust vectoring (see Append. A4).

2.3 Maneuvering Flight

MIL-STD-1797 requires that within the operational flight envelope the configuration should be able to develop, by use

of pitch control alone, load factors between $n_0(+)$ and $n_0(-)$ (maximum and minimum operational load factor). The pitch controller deflection required for the maneuvers must not exceed its range of effectiveness. Assuming the airplane is performing a pull-up from a trimmed 1-g level flight the following equations (derived based on the discussion in Section 6.10 of Ref. 6) can be used to determine the change in AOA and the additional elevator deflection angle required to achieve the desired load factor:

$$(n_z-1) \left[\frac{W}{\bar{q}S} - C_{L\alpha} \frac{g\bar{c}}{2V^2} \right] = C_{L\alpha} \Delta\alpha + C_{L\delta E} \Delta\delta E \quad (8)$$

$$-(n_z-1) C_{m\alpha} \frac{g\bar{c}}{2V^2} = C_{m\alpha} \Delta\alpha + C_{m\delta E} \Delta\delta E \quad (9)$$

2.4 Short Period and CAP requirements

The requirement is to achieve level-1 flying quality for the equivalent (with augmentation) short period damping requirements and satisfy the control anticipation parameter (CAP) requirement in Figure 1 according to the Section 4.2.1.2 of Ref. 4. The following short-period approximation equations (based on Eq. 4.80 & 4.81 of Ref. 7) can be used to estimate non-augmented flight characteristics:

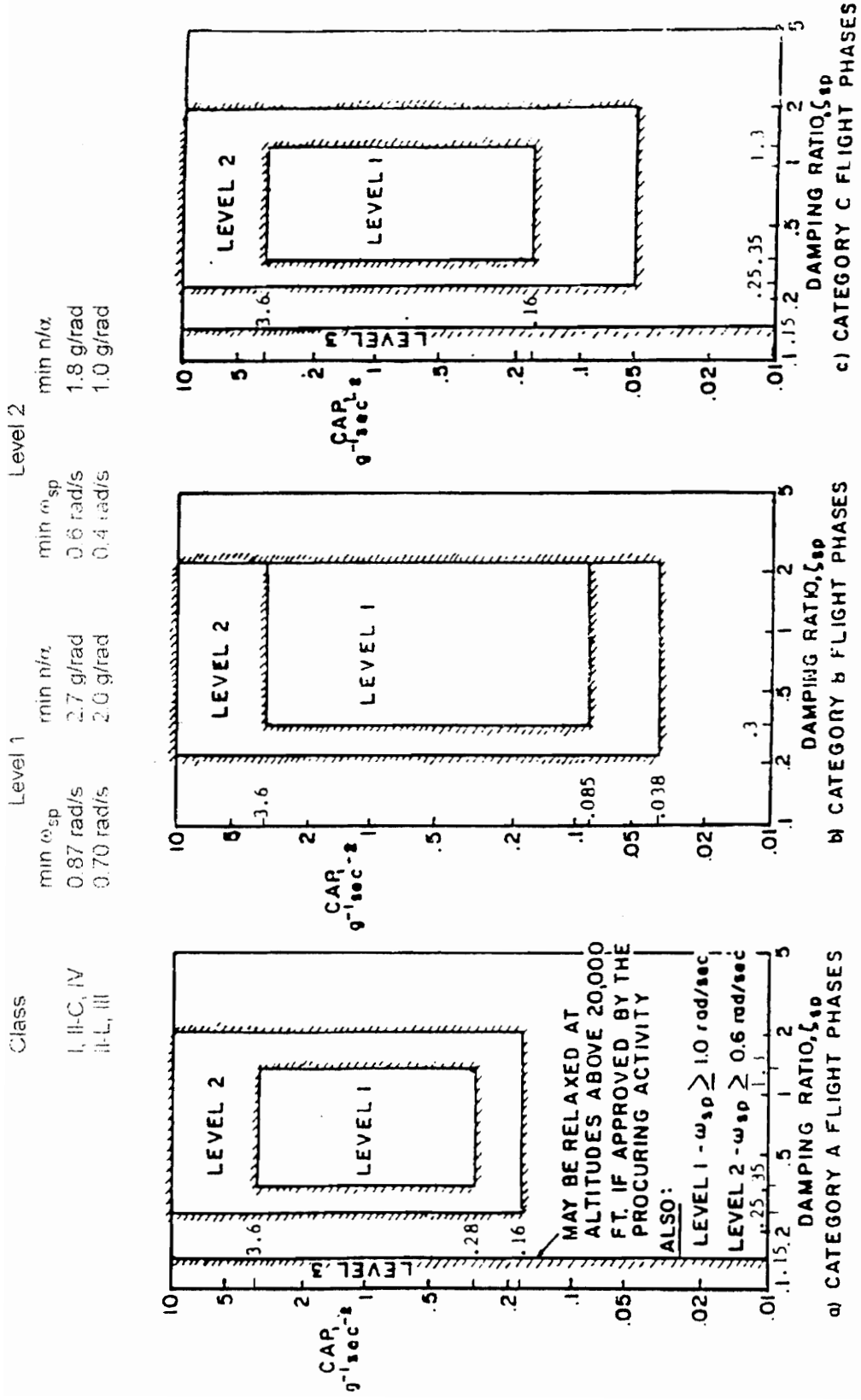


Figure 1. MIL-STD-1797 Short Period Dynamics Requirements

$$\omega_{n_{sp}} = \left[-C_{m_q} C_{L_w} \frac{(\overline{CS\bar{q}})^2}{2V^2 m I_y} - \frac{C_{m_w} \overline{CS\bar{q}}}{I_y} \right]^{\frac{1}{2}} \quad (10)$$

$$\zeta = -\frac{1}{2\omega_{n_{sp}}} \left[(C_{m_w} + C_{m_q}) \frac{\overline{C^2 S \bar{q}}}{2V I_y} - C_{L_w} \frac{\overline{qS}}{mV} \right] \quad (11)$$

Note Eq. 10 & 11 are intended for non-augmented airplanes. Aircraft with longitudinal stability augmentation (such as unstable airplanes) must account for the dynamics of the control system.

In addition, according to the definitions in Section 4.2.1.2 of Ref. 4:

$$n/\alpha = \frac{C_{L_w} \overline{qS}}{W} \quad (12)$$

$$CAP = \frac{\omega_{n_{sp}}^2}{n/\alpha} \quad (13)$$

It should be noted that some configurations simply do not fit the standard list, and there continue to be debates between experts about the adequacy and the merits of these requirements. Although this requirement is not specifically related to any control surface, horizontal tail volume strongly influences the value of the pitch rate damping coefficient.

2.5 Pitch due to Velocity Axis Roll

The aircraft concept must also possess sufficient nose-down pitch authority to compensate for the nose-up moment as a result of inertial cross-coupling during high angle-of-attack stability axis roll maneuvers (Ref. 8). Assuming the flight path is confined to a straight line without sideslip, without variations in speed, the pitching moment due to velocity axis roll can be estimated from (Ref. 9):

$$M_{couple} = P^2 \left[\frac{1}{2} (I_z - I_x) \sin(2\alpha) \right] \quad (14)$$

where P is the velocity-axis roll rate, and α , I_x and I_z are measured with respect to the principal axes system. This nose-up moment due to coupling reaches its maximum at AOA = 45 degrees. The pitch control deflection required to compensate for the roll coupling can be estimated from:

$$\delta E_{couple} = \frac{-M_{couple}}{C_{m\dot{\alpha}} \bar{c} S \bar{q}} \quad (15)$$

Note that this requirement of M_{couple} does not address the pitch authority needed to maintain attitude with zero roll rate. For unstable aircraft, the situation may be most critical around the pinch point, which is the angle of attack where the margin for nose-down moment is at its minimum.

2.6 Steady Sideslip

This requirement demands the design to have adequate roll and yaw power to perform steady sideslip maneuvers. This can become significant during cross-wind landing when the sideslip angle is the greatest because of low airspeed. To maintain steady sideslip, the net sideforce, rolling and yawing moment must vanish. The following equations (rewritten from Eq. 10.4,3 of Ref. 6) can be used to approximate the roll and yaw deflections needed to maintain sideslip:

$$\delta R = \beta \frac{-C_{n_{\delta A}} C_{l_{\beta}} + C_{l_{\delta A}} C_{n_{\beta}}}{C_{l_{\delta R}} C_{n_{\delta A}} - C_{n_{\delta R}} C_{l_{\delta A}}} \quad (16)$$

$$\delta A = \beta \frac{C_{n_{\delta R}} C_{l_{\beta}} - C_{l_{\delta R}} C_{n_{\beta}}}{C_{l_{\delta R}} C_{n_{\delta A}} - C_{n_{\delta R}} C_{l_{\delta A}}} \quad (17)$$

The resulting bank angle can be determined using:

$$\phi = - \frac{C_{y_{\beta}} \beta + C_{y_{\delta R}} \delta R}{\frac{W}{qS} \cos(\gamma)} \quad (18)$$

Generally, it is sufficient to demonstrate that no more than 75% of the roll and yaw control authority be devoted to maintaining steady sideslip. However, this requirement does not address aircraft sensitivity to lateral gust.

2.7 Engine-Out Trim

For multi-engine airplanes, the roll and yaw controllers must be sufficiently powerful to cope with asymmetric propulsion failure. Similar to steady sideslip, this requirement becomes most demanding when operating at very low speed. To maintain steady straight flight, the roll and yaw controllers must counter the effect of asymmetric thrust to produce zero sideforce and no rolling and no yawing moments. The following system of equations (derived based on the addition of asymmetric thrust contribution to Eq. 10.4,2 of Ref. 6 which are the sideforce, roll and yaw moment equations) must be simultaneously satisfied:

$$C_y=0=C_{y\beta}\beta+\frac{W}{qS}\cos(\gamma)\phi+C_{y\delta R}\delta R+C_{y_T}\Delta T \quad (19)$$

$$C_l=0=C_{l\beta}\beta+C_{l\delta R}\delta R+C_{l\delta A}\delta A+C_{l_T}\Delta T \quad (20)$$

$$C_n=0=C_{n\beta}\beta+C_{n\delta R}\delta R+C_{n\delta A}\delta A+C_{n_T}\Delta T \quad (21)$$

The unknowns to be determined are the sideslip angle and the aileron and rudder deflections. Because of control power limitations, the achievable bank angle may be limited to a certain range, ie, wings-level attitude may not be possible. It is recommended that no more than 75% of the yaw and roll control be allocated to compensate for asymmetric loss of thrust.

2.8 Time-to-Bank

The roll response to full roll control input must meet the performance requirements prescribed by Section 4.5.8.1 of MIL-STD-1797. The input is to be abrupt, with time measured from the application of force. The requirements vary depending on the class of airplane. For class IV aircraft, the pitch control is to be held fixed while the yaw control pedals shall remain free throughout the maneuver. The roll performance requirements for class IV aircraft are listed in tables 1a to 1d, and use speed ranges defined below for level-1 flying quality:

VL	$V_{o_{min}} < V < V_{min} + 20 \text{ kts}$
L	$V_{min} + 20 \text{ kts} < V < 1.4 V_{min}$
M	$1.4 V_{o_{min}} < V < .7 V_{max}$
H	$.7 V_{max} < V < V_{o_{max}}$

Because requirements of Table 1b, 1c and 1d apply to air-to-air and air-to-ground combat flight phase with more stringent guidelines, they take precedence over the requirements of Table 1a. Roll maneuvers specified in Tables 1b are to be initiated at 1-g while those specified in Tables 1a, 1c & 1d are to be initiated at load factors between $0.8n_0(-)$ and $0.8n_0(+)$. The roll performance requirements for Class IV airplane in Ground Attack flight phase with large complements of external stores may be relaxed from Table 1b (but not beyond those stated in Table 1d) with the approval of

Table 1a. General Roll Performance for Class IV Airplanes.

Level	Speed Range	Time to Achieve Bank Angle Change (sec)				
		CAT A			CAT B	CAT C
		30 deg	50 deg	90 deg	90 deg	30 deg
1	VL	1.1			2.0	1.1
	L	1.1			1.7	1.1
	M			1.3	1.7	1.1
	H		1.1		1.7	1.1
2	VL	1.6			2.8	1.3
	L	1.5			2.5	1.3
	M			1.7	2.5	1.3
	H		1.3		2.5	1.3
3	VL	2.6			3.7	2.0
	L	2.0			3.4	2.0
	M			2.6	3.4	2.0
	H		2.6		3.4	2.0

Table 1b. Air-to-Air Combat Roll Performance Requirements (Initial Load Factor = 1 G)

Level	Speed Range	Time to Achieve Bank Angle Change (sec)			
		30 deg	90 deg	180 deg	360 deg
1	VL	1.0			
	L		1.4	2.3	4.1
	M		1.0	1.6	2.8
	H		1.4	2.3	4.1
2	VL	1.6			
	L	1.3			
	M		1.3	2.0	3.4
	H		1.7	2.6	4.4
3	VL	2.5			
	L	2.0			
	M		1.7	3.0	
	H		2.1		

Table 1c. Air-to-Air Combat Roll Performance Requirements

Level	Speed Range	Time to Achieve Bank Angle Change (sec)			
		30 deg	50 deg	90 deg	180 deg
1	VL	1.0			
	L		1.1		
	M			1.1	2.2
	H		1.0		
2	VL	1.6			
	L	1.3			
	M			1.4	2.8
	H		1.4		
3	VL	2.5			
	L	2.0			
	M			1.7	3.4
	H		1.7		

Table 1d. Ground Attack Roll Performance Requirements

Level	Speed Range	Time to Achieve Bank Angle Change (sec)			
		30 deg	50 deg	90 deg	180 deg
1	VL	1.5			
	L		1.7		
	M			1.7	3.0
	H		1.5		
2	VL	2.8			
	L	2.2			
	M			2.4	4.2
	H		2.4		
3	VL	4.4			
	L	3.8			
	M			3.4	6.0
	H		3.4		

the procuring activity.

Considering one-degree of freedom motion, the following ordinary differential equations represent the rolling motion:

$$\frac{d\phi}{dt} = p \quad (22)$$

$$\frac{dp}{dt} = \frac{\bar{q}S}{I_x} [(C_{l_{\delta A}} \delta A) + (C_{l_p} p) (\frac{b}{2V})] \quad (23)$$

This system of ordinary differential equations can be numerically integrated to show compliance with requirements. One should note that this approximation does not consider the rudder deflection needed to maintain coordinated rolling motion (to be discussed in Section 2.9). In this analysis, the time scale might be small enough to warrant including the roll controller rate limit in the estimation. Assuming the maximum aileron servo rate is a constant, the actual aileron surface deflection prior to reaching the maximum position is:

$$\delta A = (\frac{\delta A}{dt})_{\max} (t - t_0) \quad \text{for } t_0 < t < t' \quad (24)$$

$$\delta A = \delta A_{\max} \quad \text{for } t > t' \quad (25)$$

$$t' = \frac{\delta A_{\max}}{(\frac{d\delta A}{dt})_{\max}} \quad (26)$$

t' is the time between roll input to the time the ailerons

reach their maximum deflection. Typically, this is only a significant factor during the initial instant of the roll input. An alternative representation of the aileron deflection can be used:

$$\delta A = (1 - e^{-\frac{t}{T}}) \delta A_{command}$$

where T is the 1st order time constant associated with the lag between the actual aileron deflection and the step aileron deflection command. Note the bank angle also can be obtained by analytically integrating Eq. 22 & 23 after substituting in the aileron deflection in Eq. 27.

2.9 Rolling Pullout

The yaw controller must possess adequate authority to overcome the yawing moment as a result of inertia coupling during a rolling pullout maneuver. According to Eq. 1 of Appendix E of Ref. 10 (derived from the total yawing moment equation), the adverse yawing moment coefficient in a rolling pullout can be approximated from:

$$C_{n_{couple}} = \frac{(I_x - I_y) \cos(\alpha) p q}{\bar{q} S b} \quad (28)$$

The pitch rate q is determined by the bank angle of the aircraft and the normal load factor applied to the airframe.

The adverse yawing moment is most severe (result of highest pitch rate, q) when the loading occurs while the airplane is inverted (due to the additional contribution from gravity). The pitch rate of the aircraft in this orientation is:

$$q = \frac{(n_z + 1)g}{V} \quad (29)$$

Combining Eq. 28 and 29, the rudder deflection needed to counter the adverse yawing moment during a pullout maneuver can be obtained from:

$$C_{n_{\delta R}} \delta R = - \frac{(I_x - I_y) \cos(\alpha) p (n_z + 1) g}{\bar{q} S b V} \quad (30)$$

2.10 Coordinated Stability Axis Roll and Roll Acceleration

To perform coordinated stability-axis rolls, both roll and yaw controllers are used to maintain zero sideslip. At low angles-of-attack there is usually adequate rudder power to obtain the desired motion. However, as the angle-of-attack increases, the demand on rudder authority increases rapidly. Consider the stability-axis roll rate (p) and roll acceleration (\dot{p}), AOA, and normal load factor as specified requirements. Resolving the forces and moments in the principal body axes system and expanding the aerodynamically generated rolling and yawing moments, Eq. a & c of 5.8,3 of

Etkin (Ref. 6) which involve the rolling and yawing moments can be rewritten as:

$$L_{\delta R}\delta R+L_{\delta A}\delta A=-(L_p\cos\alpha+L_r\sin\alpha)p+\cos\alpha\dot{p}-\frac{(I_y-I_z)}{(I_x)}\sin\alpha pq \quad (31)$$

$$N_{\delta R}\delta R+N_{\delta A}\delta A=-(N_p\cos\alpha+N_r\sin\alpha)p+\sin\alpha\dot{p}-\frac{(I_x-I_y)}{(I_z)}\cos\alpha pq \quad (32)$$

The rudder and aileron deflections are found by solving Eq. 31 & 32 simultaneously. This problem can be reformulated into the rolling pullout maneuver. Again, the most critical control power demand due to pitch rate arises when the maneuver occurs while the airplane is inverted. Similar to the rolling pullout, the conservative approach is to define pitch rate (q) as:

$$q=(n_z+1)\frac{g}{v}. \quad (33)$$

2.11 High Angle-of-Attack Departure

This section identifies some parameters that are found to be useful in determining the susceptibility of departure during high AOA operation. However, the inability to estimate high AOA aerodynamic characteristics makes it difficult to assess the stability and control authority requirements at high angle of attack in the conceptual design stage.

Therefore, high-AOA stability is not included as part of the control power assessment methodology for conceptual designs. Many parameters have been proposed as the measure of departure tendency. An overview of the connection between various proposed criteria and the related theoretical foundation has been given recently by Lutze et al (Ref. 11). Although not ideal, two are commonly used.

While not directly related to control power, the open-loop directional stability can be roughly evaluated from $C_{n_{\beta_{eff}}}$:

$$C_{n_{\beta_{eff}}} = C_{n_{\beta}} \cos \alpha - \frac{I_z}{I_x} C_{l_{\beta}} \sin \alpha. \quad (34)$$

Note that $C_{n_{\beta}}$ and $C_{l_{\beta}}$ are in principal axis. Aircraft with positive values for this parameter tend to exhibit little yaw departure tendency.

The second (closed-loop) parameter frequently used to measure departure tendency is the Lateral Control Departure Parameter (LCDP):

$$LCDP = C_{n_{\beta}} - \frac{C_{n_{\beta A}}}{C_{l_{\beta A}}} C_{l_{\beta}}. \quad (35)$$

A value of LCDP greater than zero generally indicates that the configuration tends to be spin resistant (Ref. 8) and less susceptible to aileron induced departure (Ref. 12).

Despite suggestions by Chody et al. (Ref. 8) and Bihrlé & Barnhart (Ref. 13) of the imperfection of using these two parameters as design figures of merits, they continue to be used to assess lateral departure tendency at high angle-of-attack (Ref. 8).

3. Discussion of Overall Assessment Methodology

The goal of this control authority assessment methodology is to evaluate a given design concept during the conceptual and preliminary design stage against the requirements of the potentially critical maneuvers and flight conditions listed in Section 2. Figure 2 outlines the procedure involved to complete the task.

For each requirement discussed in Section 2, there is a set of combinations of flight condition variables such as weight, CG location, load factor, altitude and speed, that affect the performance of the airplane. Therefore the methodology must evaluate the configuration's control power under conditions that place the greatest demand on control power. For example, when checking the nose-wheel lift-off capability of a configuration, maximum gross takeoff weight with most forward CG location will define the most critical nose-up pitch authority condition. It is important to perform the control authority analysis with these critical flight condition variables so that the most severe cases are tested.

With the airplane geometry and the flight condition variables corresponding to each requirement, one needs to obtain the necessary aerodynamic characteristics in the form of stability and control derivatives. Unfortunately, early in the preliminary design phase, wind tunnel data usually is not available. Therefore, US Air Force Stability & Control DATCOM

Control Authority Assessment Methodology

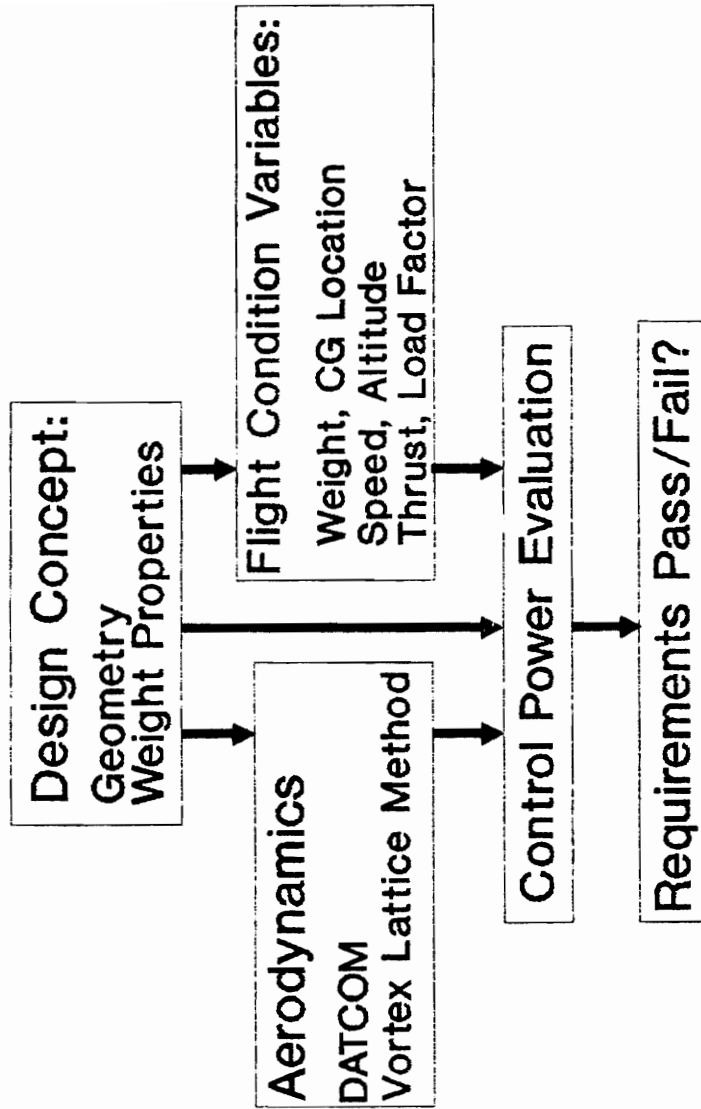


Figure 2. Control Authority Assessment Methodology

type methodology (Ref. 1) is the typical method used in estimating aerodynamic properties. However, this process can be very time consuming, and may not be applicable to all geometric arrangements of interest. With the availability of ever-increasing computing capability, computational aerodynamics can be incorporated to expedite the process of estimating stability and control derivatives. In this study, a subsonic vortex-lattice method is adapted to supplement DATCOM in estimating subsonic, low angle of attack aerodynamic characteristics.

The estimated stability and control derivatives along with the corresponding flight conditions are then applied to the airplane dynamics equations examined in Section 2. The results typically are in the form of control surface deflections which are indications of how much of the available control authority is used. At this point in the analysis, one must judge whether the deflections are acceptable. In the cases of nose-wheel lift-off and time-to-bank performance requirements, one must check whether the maneuvers can be accomplished according to the specifications. For short period & CAP requirements, the configuration must demonstrate flight characteristics within the defined tolerance. Note that Equations 10 & 11 outlined in Section 2.4 cannot be used for unstable configurations. If the vehicle is unstable, it is assumed that stability augmentation will be used, and the

control system is designed to satisfy the flight characteristic requirements.

If the design concept fails to meet some of the requirements, the designer must adjust the configuration in terms of sizing, geometry, weight properties, and/or relax the performance requirements. Generally, increasing control authority by geometry changes alone to satisfy certain performance requirements may not always be practical due to the resulting weight and drag penalties. If any changes are made, the new design's control power must be re-evaluated.

3.1 Flight Conditions Variables

For a design concept there are variables independent of aerodynamic properties that can change the demands on control authority. These parameters vary considerably as functions of flight phase category and store configuration. The objective of this section is to qualitatively identify the variables of each requirement that can lead to the need for large control authority. The variables to be considered are:

- Weight
- Inertias
- C.G. Location
- Engine Thrust
- Thrust Deflection Angle(s)
- Load Factor
- Altitude
- Speed

Note that not all of these variables need to be specified for

each requirement evaluation.

For the nose-wheel lift-off requirement, airplane weight should be the maximum gross takeoff weight with CG located at its most forward position. Use of the maximum value of I_y with maximum thrust at sea level should lead to a conservative estimation. Future advanced aircraft may employ thrust vectoring to shorten the ground roll distance during takeoff. On the one hand, pointing the thrust (jet exhaust) upward (for aft-engine configurations) decreases the nose-wheel lift-off speed by providing additional nose-up moment but leads to increased downward force. On the other hand, diverting the exhaust downward adds to the total lift but requires additional nose-up control authority from another pitch controller. Therefore, thrust deflections at both extremes should be examined. Similar combinations of variables should to be used for landing, while reducing the airplane weight to maximum landing weight.

For 1-G trim requirements, the analysis should be performed at all corners of the operational 1-G V-h diagram with particular emphasis near the stall boundary. CG locations at both extremes should be considered.

In the maneuvering flight requirement analysis, variation of load factors, speed, altitude, and weight are most significant. While it is conservative to use maximum weight in conjunction with maximum load factor, structural limits may

not allow such condition to occur. It is important to explore all boundaries of the V-h diagram for all load factors, with special emphasis in the low speed regime.

For short period & CAP specifications, Mach number and CG location can significantly influence the flying qualities. However, it is impractical and unnecessary to examine all possible combinations. Emphasis should be placed at the nominal design points. One should keep in mind that the actual flying qualities may be significantly different from the prediction here for highly augmented airplanes.

Three of the flight condition variables are important in evaluating pitch control effectiveness against roll-induced pitch-up. Maximum I_z and minimum I_x should be used. While low speed tends to result in saturating the pitch controller, high roll rate usually does not occur near this regime. Therefore speeds between the range of L and H (as defined in Section 2.8) should be used for the test.

Achieving a large sideslip angle is usually most critical during landing approach. Evaluation of this requirement should be carried out at minimum landing speed. Lateral thrust vectoring angle (if available) should be varied to reduce the burden on the yaw controller or produce the worst-case scenario.

Antisymmetric thrust becomes most critical during low-speed operations. Minimum speed and maximum asymmetric thrust

should be considered in the analysis. If lateral thrust vectoring is available, it should be directed so that the thrust line passes through CG to alleviate the burden on the yaw controller.

For time-to-bank performance evaluation, the range of speed defined in Section 2 should be considered. The lowest value of each of the four speed ranges defined in Section 2.8 should be used in the analysis. In addition, I_x should assume the largest value corresponding to the flight phase under consideration to produce conservative estimates.

In the case of the rolling pullout maneuver and a coordinated roll, the largest adverse yawing moment is produced when the difference between the values of I_x and I_y are the largest. Therefore the minimum I_x and maximum I_y and I_z should be used in the analyses. Because high stability axis roll rate and high load factors are not possible at very low speeds, speed ranges between L and H should be used while applying maximum load factor allowed by the speeds to produce the most critical conditions.

A FORTRAN program, FLTCOND, was written with a spreadsheet (see Figure 3) as input to help accelerate the process of isolating the most critical combinations of flight condition variables for each requirement. A typical output of FLTCOND is shown in Table 2. The flight condition variable, such as CG location, inertias, etc., listed are to be used in

the final control authority assessment check. It simply serves to provide candidate combinations of flight condition variables that may result in the most critical demand on control power for each requirement. However, it may, for some cases, be too stringent and repetitive. The user must make the necessary adjustment based on the overall design objectives.

CONTROL POWER ASSESSMENT PROGRAM

Part 1. Flight Condition Variables

Prepared by Jacob Kay Feb. 1992

Variables	Units	Value
Minimum Gross Weight	(lbs)	25000
Maximum Gross Weight	(lbs)	45000
Minimum I-x	(slug-ft ²)	23168
Maximum I-x	(slug-ft ²)	80000
Minimum I-y	(slug-ft ²)	100000
Maximum I-y	(slug-ft ²)	123936
Minimum I-z	(slug-ft ²)	120000
Maximum I-z	(slug-ft ²)	200000
Most Forward C.G. Location	(ft)	31.5
Most Aft C.G. Location	(ft)	32.5
Max. Thrust with Thrust Vectoring	(lbs)	35000
Max. Thrust w/o Thrust Vectoring	(lbs)	25000
Max. Thrust Deflection Angle--Up	(deg)	20
Max. Thrust Deflection Angle--Down	(deg)	15
Max. Thrust Deflection Angle--Yaw	(deg)	10
Maximum Normal Load Factor	(g's)	9.5
Altitude/Speed Range:		
Number of Entries:		5
Altitude	(ft)	0
Minimum Speed	(knots)	130
Maximum Speed	(knots)	890
Altitude	(ft)	10000
Minimum Speed	(knots)	180
Maximum Speed	(knots)	992
Altitude	(ft)	20000
Minimum Speed	(knots)	220
Maximum Speed	(knots)	998
Altitude	(ft)	30000
Minimum Speed	(knots)	240
Maximum Speed	(knots)	1001
Altitude	(ft)	45000
Minimum Speed	(knots)	280
Maximum Speed	(knots)	1020

Figure 3. Sample Input Spreadsheet for program FLTCOND

Table 2. Sample Output of Program FLTCOND.

Note: Entries of .900E+16 indicate that the variable does not need to be explicitly specified.

NOSE-WHEEL LIFT-OFF

W (lbs)	I-x	I-y	I-z	Xcg (ft)	T (lbs)	Load Factor	ALT (ft)	Spd (kts)	VT DEF	HT Def(deg)
519E+05	.900E+16	.140E+06	.900E+16	.311E+02	.337E+05	.900E+16	.000E+00	.900E+16	.000E+00	.000E+00

LANDING.

W (lbs)	I-x	I-y	I-z	Xcg (ft)	T (lbs)	Load Factor	ALT (ft)	Spd (kts)	VT DEF	HT Def(deg)
519E+05	.900E+16	.140E+06	.900E+16	.311E+02	.900E+16	.100E+01	.000E+00	.900E+16	.000E+00	.000E+00

1-G TRIM.

W (lbs)	I-x	I-y	I-z	Xcg (ft)	T (lbs)	Load Factor	ALT (ft)	Spd (kts)	VT DEF	HT Def(deg)
519E+05	.900E+16	.900E+16	.900E+16	.311E+02	.900E+16	.100E+01	.000E+00	.120E+03	.000E+00	.000E+00
519E+05	.900E+16	.900E+16	.900E+16	.311E+02	.900E+16	.100E+01	.000E+00	.100E+04	.000E+00	.000E+00
384E+05	.900E+16	.900E+16	.900E+16	.320E+02	.900E+16	.100E+01	.500E+05	.326E+03	.000E+00	.000E+00
384E+05	.900E+16	.900E+16	.900E+16	.320E+02	.900E+16	.100E+01	.500E+05	.103E+04	.000E+00	.000E+00

MANEUVERING FLIGHT:

W (lbs)	I-x	I-y	I-z	Xcg (ft)	T (lbs)	Load Factor	ALT (ft)	Spd (kts)	VT DEF	HT Def(deg)
519E+05	.900E+16	.900E+16	.900E+16	.311E+02	.900E+16	.150E+01	.000E+00	.120E+03	.000E+00	.000E+00
519E+05	.900E+16	.900E+16	.900E+16	.311E+02	.900E+16	.900E+01	.000E+00	.100E+04	.000E+00	.000E+00
384E+05	.900E+16	.900E+16	.900E+16	.320E+02	.900E+16	.150E+01	.500E+05	.326E+03	.000E+00	.000E+00
384E+05	.900E+16	.900E+16	.900E+16	.320E+02	.900E+16	.855E+01	.500E+05	.103E+04	.000E+00	.000E+00

SHORT PERIOD & CAP REQUIREMENTS:

Perform evaluation at design points:

PITCH DUE TO STABILITY AXIS ROLL

W (lbs)	I-x	I-y	I-z	Xcg (ft)	T (lbs)	Load Factor	ALT (ft)	Spd (kts)	VT DEF	HT Def(deg)
.900E+16	.200E+05	.900E+16	.220E+06	.320E+02	.900E+16	.900E+16	.000E+00	.120E+03	.000E+00	.000E+00
.900E+16	.200E+05	.900E+16	.220E+06	.320E+02	.900E+16	.900E+16	.000E+00	.560E+03	.000E+00	.000E+00
.900E+16	.200E+05	.900E+16	.220E+06	.320E+02	.900E+16	.900E+16	.000E+00	.100E+04	.000E+00	.000E+00
.900E+16	.200E+05	.900E+16	.220E+06	.320E+02	.900E+16	.900E+16	.100E+05	.160E+03	.000E+00	.000E+00
.900E+16	.200E+05	.900E+16	.220E+06	.320E+02	.900E+16	.900E+16	.100E+05	.655E+03	.000E+00	.000E+00
.900E+16	.200E+05	.900E+16	.220E+06	.320E+02	.900E+16	.900E+16	.100E+05	.115E+04	.000E+00	.000E+00
.900E+16	.200E+05	.900E+16	.220E+06	.320E+02	.900E+16	.900E+16	.500E+05	.326E+03	.000E+00	.000E+00
.900E+16	.200E+05	.900E+16	.220E+06	.320E+02	.900E+16	.900E+16	.500E+05	.679E+03	.000E+00	.000E+00
.900E+16	.200E+05	.900E+16	.220E+06	.320E+02	.900E+16	.900E+16	.500E+05	.103E+04	.000E+00	.000E+00

TIME-to-BANK PERFORMANCE

W (lbs)	I-x	I-y	I-z	Xcg (ft)	T (lbs)	Load Factor	ALT (ft)	Spd (kts)	VT DEF	HT Def(deg)
.900E+16	.390E+05	.900E+16	.220E+06	.320E+02	.900E+16	.100E+01	.000E+00	.120E+03	.000E+00	.000E+00
.900E+16	.390E+05	.900E+16	.220E+06	.320E+02	.900E+16	.100E+01	.000E+00	.413E+03	.000E+00	.000E+00
.900E+16	.390E+05	.900E+16	.220E+06	.320E+02	.900E+16	.100E+01	.000E+00	.707E+03	.000E+00	.000E+00
.900E+16	.390E+05	.900E+16	.220E+06	.320E+02	.900E+16	.100E+01	.000E+00	.100E+04	.000E+00	.000E+00
.900E+16	.390E+05	.900E+16	.220E+06	.320E+02	.900E+16	.100E+01	.100E+05	.160E+03	.000E+00	.000E+00
.900E+16	.390E+05	.900E+16	.220E+06	.320E+02	.900E+16	.100E+01	.100E+05	.490E+03	.000E+00	.000E+00
.900E+16	.390E+05	.900E+16	.220E+06	.320E+02	.900E+16	.100E+01	.100E+05	.820E+03	.000E+00	.000E+00
.900E+16	.390E+05	.900E+16	.220E+06	.320E+02	.900E+16	.100E+01	.100E+05	.115E+04	.000E+00	.000E+00
.900E+16	.390E+05	.900E+16	.220E+06	.320E+02	.900E+16	.100E+01	.500E+05	.326E+03	.000E+00	.000E+00
.900E+16	.390E+05	.900E+16	.220E+06	.320E+02	.900E+16	.100E+01	.500E+05	.561E+03	.000E+00	.000E+00
.900E+16	.390E+05	.900E+16	.220E+06	.320E+02	.900E+16	.100E+01	.500E+05	.797E+03	.000E+00	.000E+00
.900E+16	.390E+05	.900E+16	.220E+06	.320E+02	.900E+16	.100E+01	.500E+05	.103E+04	.000E+00	.000E+00

STEADY SIDESLIP

W (lbs)	I-x	I-y	I-z	Xcg (ft)	T (lbs)	Load Factor	ALT (ft)	Spd (kts)	VT DEF	HT Def(deg)
.384E+05	.900E+16	.900E+16	.900E+16	.329E+02	.900E+16	.100E+01	.000E+00	.120E+03	.000E+00	.000E+00

ENGINE-OUT TRIM.

W (lbs)	I-x	I-y	I-z	Xcg (ft)	T (lbs)	Load Factor	ALT (ft)	Spd (kts)	VT DEF	HT Def(deg)
.248E+05	.900E+16	.900E+16	.900E+16	.329E+02	.159E+05	.100E+01	.000E+00	.120E+03	.000E+00	.000E+00
.243E+05	.900E+16	.900E+16	.900E+16	.329E+02	.159E+05	.100E+01	.000E+00	.120E+03	.000E+00	.000E+00

COORDINATED ROLL & ROLLING PULLOUT

W (lbs)	I-x	I-y	I-z	Xcg (ft)	T (lbs)	Load Factor	ALT (ft)	Spd (kts)	VT DEF	HT Def(deg)
.900E+16	.200E+05	.140E+06	.900E+16	.329E+02	.900E+16	.150E+01	.000E+00	.120E+03	.000E+00	.100E+01
.900E+16	.200E+05	.140E+06	.900E+16	.329E+02	.900E+16	.550E+01	.000E+00	.560E+03	.000E+00	.100E+01
.900E+16	.200E+05	.140E+06	.900E+16	.329E+02	.900E+16	.900E+01	.000E+00	.100E+04	.000E+00	.100E+01
.900E+16	.200E+05	.140E+06	.900E+16	.329E+02	.900E+16	.100E+01	.500E+05	.326E+03	.000E+00	.100E+01
.900E+16	.200E+05	.140E+06	.900E+16	.329E+02	.900E+16	.100E+01	.500E+05	.579E+03	.000E+00	.100E+01
.900E+16	.200E+05	.140E+06	.900E+16	.329E+02	.900E+16	.100E+01	.500E+05	.103E+04	.000E+00	.100E+01

3.2 Stability & Control Derivatives

The values of stability and control derivatives of a design configuration vary considerably depending on flight condition variables such as Mach number and CG location. Once these variables are selected, the stability and control derivatives can be estimated using US Air Force Stability & Control DATCOM type methods. The focus of this section is to describe the process involved in using the vortex-lattice method (VLM) program to calculate some subsonic stability and control derivatives. The detailed discussion of the VLM code is reserved for Section 4.

Two input files must be created; one containing the longitudinal, and the other the lateral planform of the design concept. The coordinate system used for this VLM code is shown in Figure 4. The geometry of the aircraft is composed of sections of flat trapezoids to represent the aircraft (see Figure 5). Both input files follow the format shown in Figure 6. The number in the first row must be an integer from 1 to 5, representing the number of sections to be modelled. The succeeding four lines are the cartesian coordinates for the four corner points following the order shown of the first section. The fifth line of each section contains the leading edge flap and trailing edge flap chord ratios. The control surfaces are assumed to occupy the full span of the section.

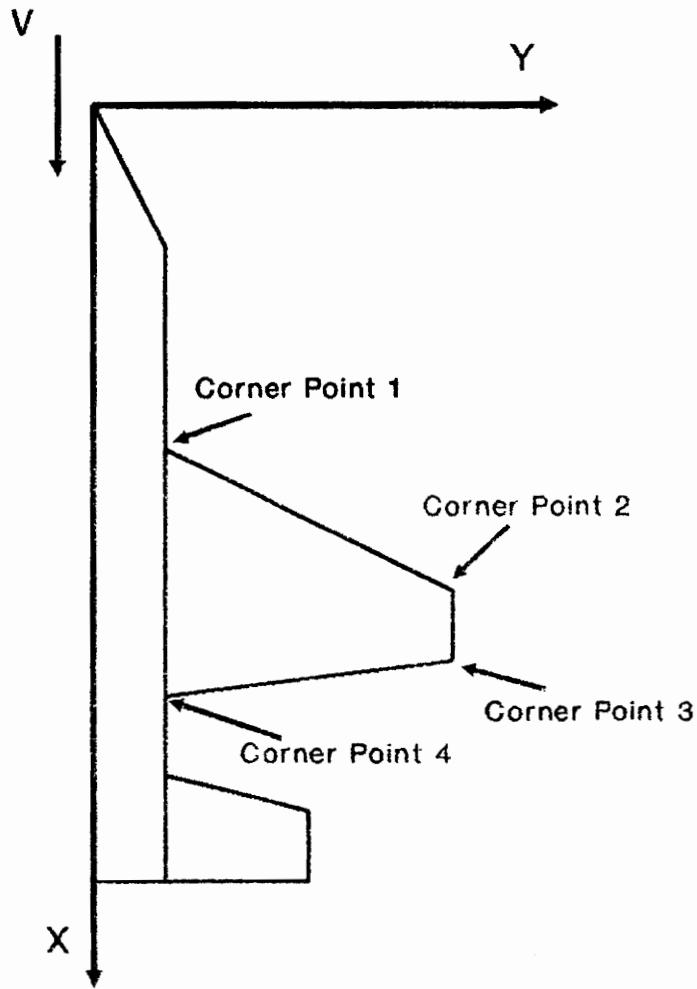


Figure 4. VLM Coordinate System

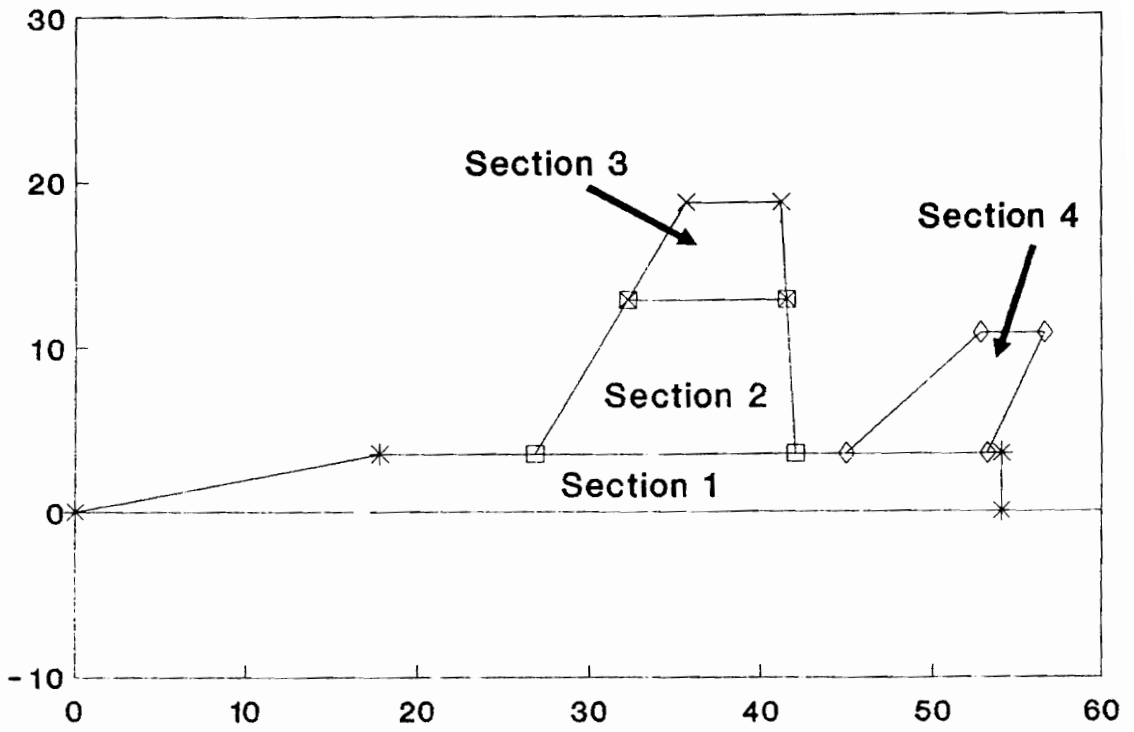


Figure 5. F-18's Longitudinal Planform Representation in VLM

Number of Sections

	X	Y	Z	
4	0.0	0.0	0.0	
	17.8	3.49	0.0	Section 1
	54.0	3.49	0.0	
	54.0	0.0	0.0	
	.00	.00		
	26.85	3.49	0.0	
	32.24	12.83	-.4895	Section 2
	41.49	12.83	-.1877	
	42.02	3.49	0.0	
	.20	.30		
	32.24	12.83	-.4895	
	35.64	18.71	-.7976	Section 3
	41.16	18.71	-.4114	
	41.49	12.83	-.1877	
	.20	.30		
	44.946	3.49	0.0	
	52.81	10.823	-.256	Section 4
	56.60	10.823	-.256	
	53.17	3.49	0.0	
	1.0	.00		

L.E. Flap Chord Ratio
T.E. Flap Chord Ratio

Figure 6. Elements of Input File to VLM Program

If a section is to represent an all-moving control surface, enter 1.0 and 0.0 for the leading edge flap and trailing edge flap chord ratio respectively. For the longitudinal case, the VLM program assumes that the configuration is symmetrical about the x-axis.

Each section is divided into 40 panels (8 streamwise and 5 spanwise). Due to memory and speed constraints, the program is limited to handle a maximum of 5 sections. Wing twist and dihedral can be modelled by entering the appropriate z-coordinate for the corner points. The program assumes that the twist distribution obeys the "straight-line wrap" rule where the hinge line is straight throughout the span of a section. Sections need not be in the same plane. For example, consider a horizontal tail in a T-tail configuration. Winglets may be modelled but must not have dihedral angles exactly equal to +90 or -90 degrees (as long as the y-coordinates of point 1 and 2 of the section are of different value). Note that corner points 1 & 4 and 2 & 3 should line up streamwise.

For lateral/directional stability analysis, the aircraft can be modelled with the side profile alone without the wing or the horizontal tail. Omitting wing and other surfaces with large dihedral angles from the model will result in excluding their contributions to the side-slip and yaw-rate derivatives. A sample geometry is shown in Figure 7. In both the

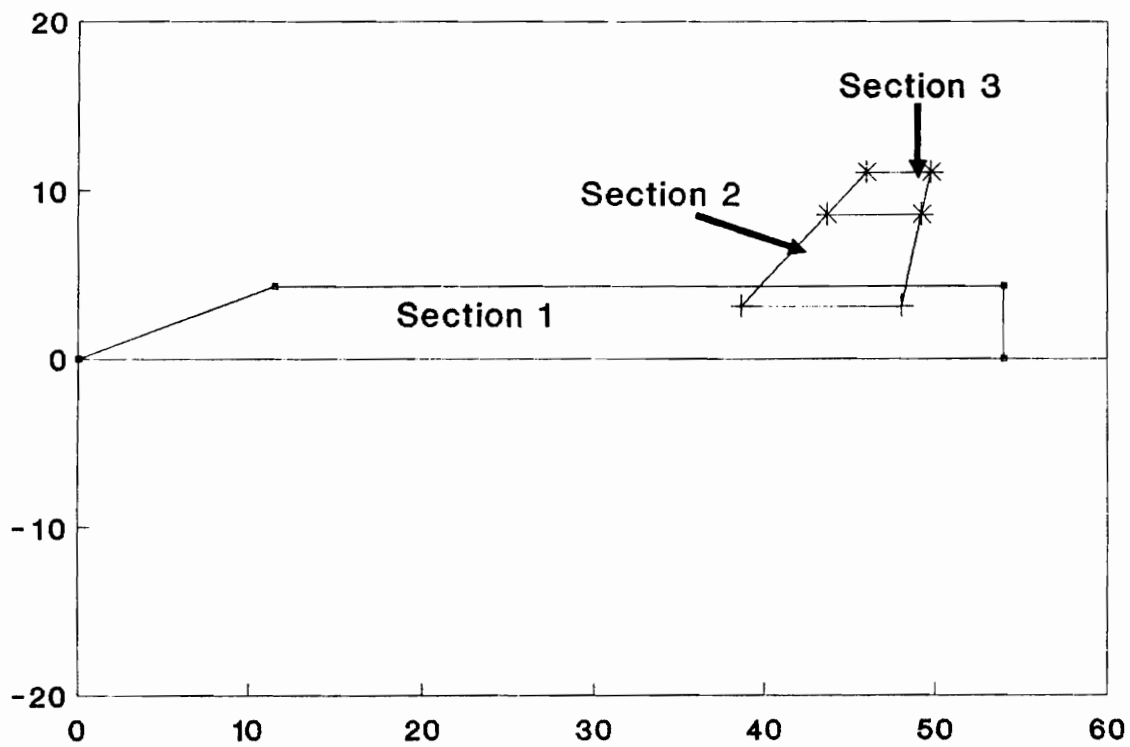


Figure 7. F-18 Lateral Profile Representation in VLM

longitudinal and lateral/directional analyses, the fuselage is approximated by a flat plate.

At the start of the program, the user is prompted to enter the Mach number, reference area, chord and span, height above the ground (for ground effect), and x- and z-coordinates of the CG location. A sample output of stability and control derivatives is shown in Figure 8. Symbols used in the VLM output file are described in the List of Symbols. Note the yawing moment caused by induced drag resulting from antisymmetric (aileron) deflection is not well-predicted by the program. However, if the configuration has a V or Y-tail, such as the YF-23, the value is valid. Some other derivatives are not well-predicted (to be discussed in Section 4.2), and the user should consider using DATCOM predictions.

At this point of the control authority assessment, there is sufficient information to apply to the governing dynamics equations identified in Section 2 to determine if the configuration possesses adequate control power.

```

HEIGHT ABOVE GROUND = 8.999999E+09
X-cg = 32.000000
MACH NUMBER = 6.000000E-01
Cl0 = -5.792204E-02
CM0 = 1.520589E-02
CDi/CL*CL = 7.817595E-02
CL-alpha = 4.245649
Cm/CL = -5.702696E-02
Lift-curve slope of tail due to downwash of wing = 6.033829E-01
CL-q = 8.579027
CM-q = -6.335838
CL-delta [2 1] = .4630E-01
Cm-delta [2 1] = .1463E+00
CL-delta [2 2] = .9674E+00
Cm-delta [2 2] = .1696E+00
CL-delta [3 1] = .2463E-01
Cm-delta [3 1] = .2127E-01
CL-delta [3 2] = 6479E+00
Cm-delta [3 2] = -3735E+00
CL-delta [4 1] = 9026E+00
Cm-delta [4 1] = -1216E+01
Cl-delta [2 1] = -6247E-02
Cn-delta [2 1] = -1571E-02
Cl-delta [2 2] = -1765E+00
Cn-delta [2 2] = -4408E-02
Cl-delta [3 1] = -5360E-02
Cn-delta [3 1] = -3322E-03
Cl-delta [3 2] = -1834E+00
Cn-delta [3 2] = .1014E-03
Cl-delta [4 1] = -1154E+00
Cn-delta [4 1] = .3306E-01
Cy-beta = -5.408736E-01
Cn-beta = 9.150367E-02
Cl-beta = -8.456216E-02
Cy-r = 5.135034E-01
Cn-r = -2.147621E-01
Cl-r = 7.204735E-02
Cl-p = -4.443568E-01
Cn-p = -1.055444E-01
Cy-delta [2 2] = -.1142E+00
Cl-delta [2 2] = -.1775E-01
Cn-delta [2 2] = .4781E-01
Cy-delta [4 2] = -.1137E+00
Cl-delta [4 2] = -.1779E-01
Cn-delta [4 2] = .4755E-01

```

Figure 8. Sample VLM Stability and Control Derivative Output

3.3 Control Power Evaluation for Requirements

Because each of the requirements may be evaluated several times under different flight conditions, a spreadsheet was constructed using LOTUS 123 to speed up the process. In general, each requirement has an input section where all pertinent variables are entered. For some requirements, intermediate calculations are performed in the Calc. section to arrive at the output. Some requirements require solving systems of linear equations. Macros are included so that simple commands from the user can initiate the necessary recalculation. For nosewheel lift-off and time-to-bank requirements, simulation of the motions are necessary. The worksheet includes numerical integrations (using Euler's method) to determine the time-dependent results. Appendix A2 contains the worksheets for each of the different requirements.

4. Vortex Lattice Method

Vortex lattice methods (VLM) are widely used for estimating the neutral point and other aircraft characteristics. They have been incorporated in conceptual airplane design to predict the configuration neutral point, lift-curve slope and lifting surface interaction. In this study, a simplified VLM is used to perform stability and control derivative estimation. Limited to subsonic flight speeds, this computational approach is better than using DATCOM in that unconventional geometric arrangements can be accommodated and the user's calculations are less time consuming. However, it is limited to analysis of subsonic flows. The Prandtl-Glauert Correction is used to account for Mach number effects. Since the VLM is based on potential flow theory, its validity is restricted to the linear aerodynamics region, and hence is valid in the low- AOA flight regime. It does not account for viscous effects. The best theoretical introduction to typical VLM schemes is in Chapter 7 of Bertin and Smith (Ref. 14).

4.1 Code Implementation: Concept and Limitations

Many variations of the vortex lattice method have been developed for various applications. The implications of the Helmholtz and Kelvin vortex theorems are that a lifting surface can be represented by a vortex sheet. The VLM scheme

used in this study is slightly unusual (typically horseshoe vortices are used instead of vortex rings) and is a direct implementation of the method presented in Section 12.3 of the recent text by Katz and Plotkin (Ref. 15). It uses a series of closed trapezoidal vortex rings to represent the airplane surfaces as illustrated in Figure 9. Note the actual vortex ring is displaced down stream by a quarter chord of each panel. The control point is located at the center of each ring, where the "non-penetration" surface boundary condition,

$$\vec{V} \cdot \vec{n} = 0 \quad (36)$$

is satisfied.

To obtain the stability derivatives, the strengths of each of the vortex rings must be found so that the vector sum of their induced velocity and the free-stream contribution at each control point satisfies the boundary condition. The induced velocity at a point due to a straight line segment of vortex filament is governed by the Biot-Savart Law. Since the Helmholtz vortex theorem says that a vortex cannot end in fluid, the vortex filament must form a closed ring (such as those representing the lifting surface) or extend to infinity (trailing horseshoe vortices in Figure 9).

The effect of compressibility is included using the Prandtl-Glauert rule as illustrated in Figure 10. This approximation stretches the x-coordinate of the distributed

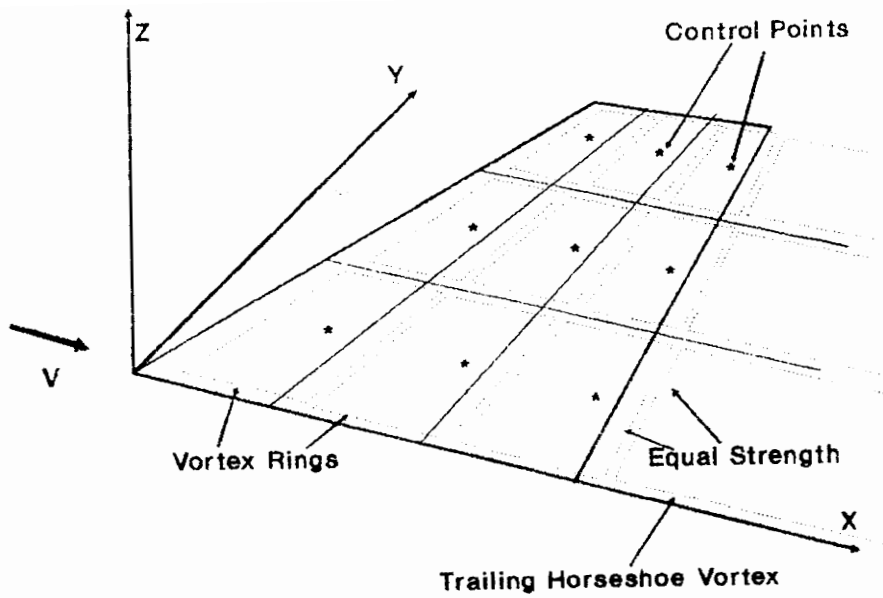


Figure 9. Vortex Rings & Control Points of VLM Implementation

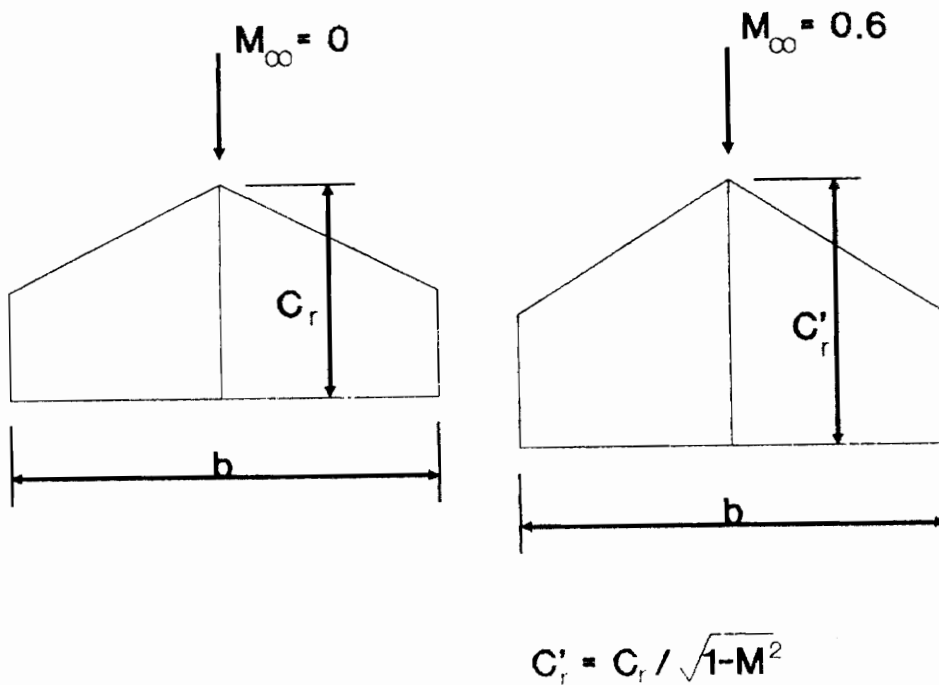


Figure 10. Prandtl-Glauert Correction Rule Used in VLM To Account for Compressibility

singularities (vortex rings, etc.) as the Mach number increases. The resulting pitching and yawing moments (now over estimated because of the elongation in the x-coordinate) are re-adjusted with the Prandtl-Glauert correction factor β . Generally, this approximation is good up to $M = 0.6$.

Differences between VLM solutions are used to estimate the various derivatives. The program first solves for the vortex strength distribution of the configuration at a reference condition, and sums the values of circulation to obtain the forces and moments. It then alters the problem by introducing a perturbation in the flow such as surface deflection or AOA change. The desired non-dimensional derivatives are then calculated by normalizing the difference of the forces or moments from those of the reference case by the magnitude of the perturbation.

To approximate pitch-, roll- and yaw-rate derivatives, an additional velocity component distribution illustrated in Figure 11 is added to the free-stream velocity at the control points. Since the program takes full advantage of symmetric flow about the x-axis, the following assumptions are made to obtain the approximate solution for asymmetric flow problems such as antisymmetric aileron deflections and roll-rate derivatives without doubling the number of equations and unknowns. First, the net lift is unchanged from that of the reference condition, and second, the change in vortex

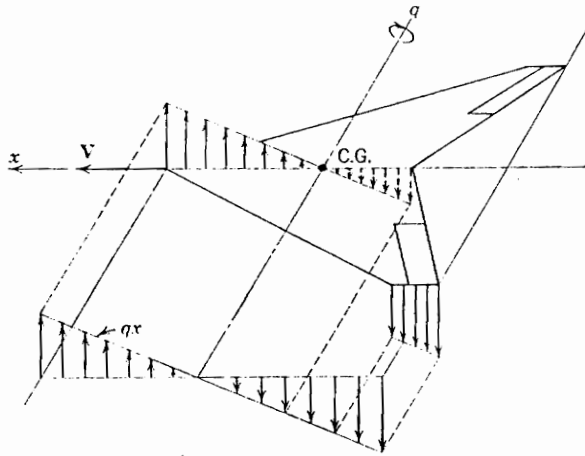


Figure 11. Surface Velocity Distribution due to Pitching Rate (from Reference 6)

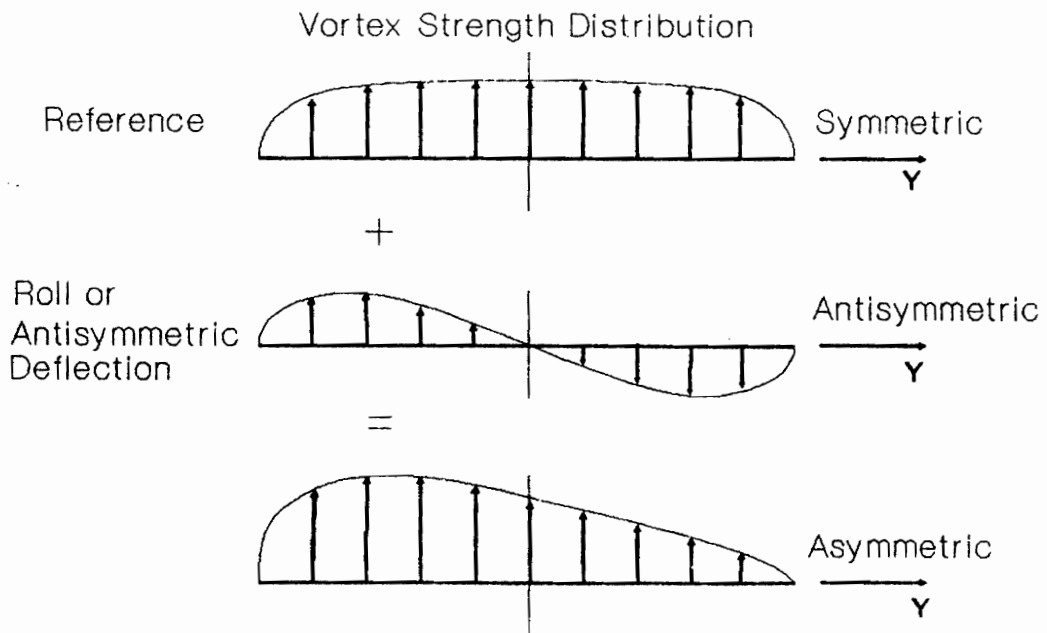


Figure 12. Spanwise Vortex Strength Distribution for Asymmetric Loading

distribution caused by the asymmetry is antisymmetric about the x-axis. Now the vortex distribution in the asymmetric flow can be decomposed into a symmetric and an antisymmetric pattern as shown in Figure 12. The symmetric distribution is already known from the reference condition, and its influence at each control point can be calculated. Under this formulation, the idea is to solve for the antisymmetric distribution alone. For each control surface listed in the longitudinal geometry file, the program first deflects it individually symmetrically to estimate its effect on the lift and pitching moment. Its effect on roll and perhaps yaw moment (such as in the case of V-tail) is then calculated using the approach discussed above.

The VLM program is also capable of performing the longitudinal stability and control derivative estimation in ground effect. The ground effect is modelled with the imaginary presence of a vortex system with opposite vortex strength distribution placed $2h$ (h is the height of the surface above the ground) below the real vortex system (see Figure 13). The number of unknowns (the strength of each vortex ring) are still the same due to the symmetry.

An F-18 model was constructed to be used for VLM validation. The resulting longitudinal and lateral/directional grid points are shown in Figure 14 and 15 respectively. Four sections are used to represent the

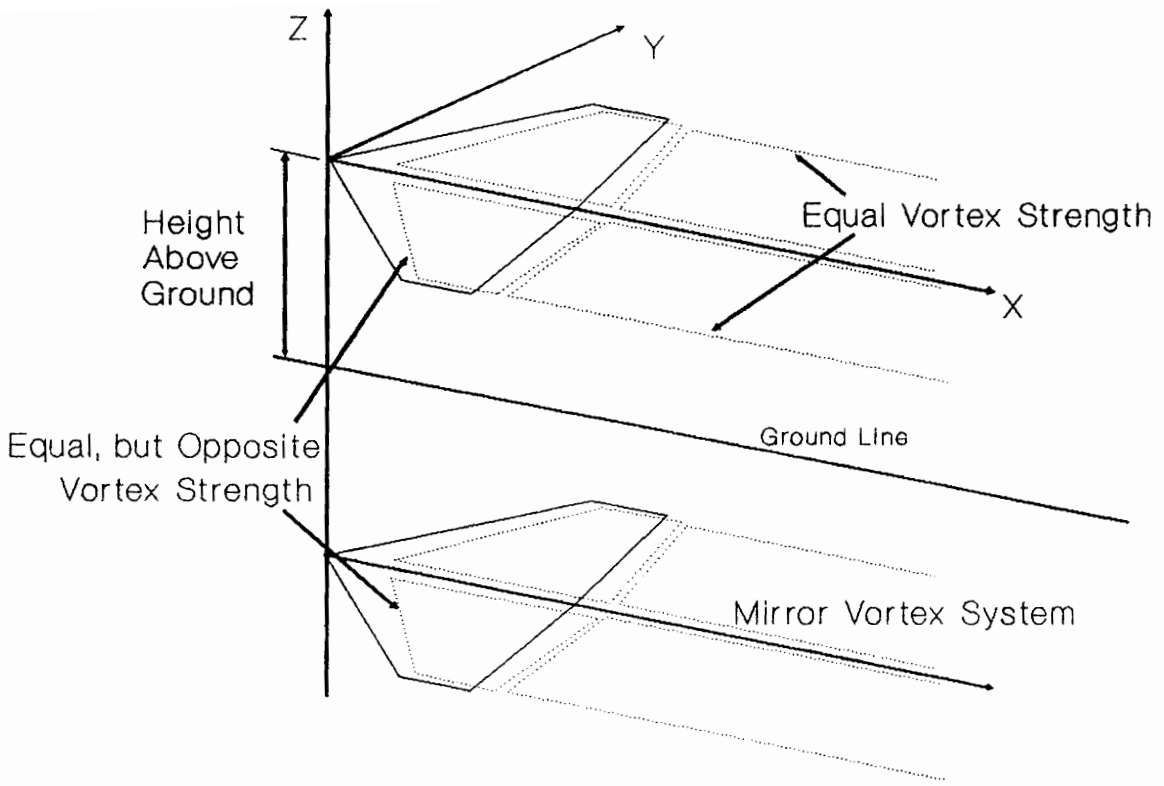


Figure 13. Use of Mirror Vortex System to Model Ground Effect

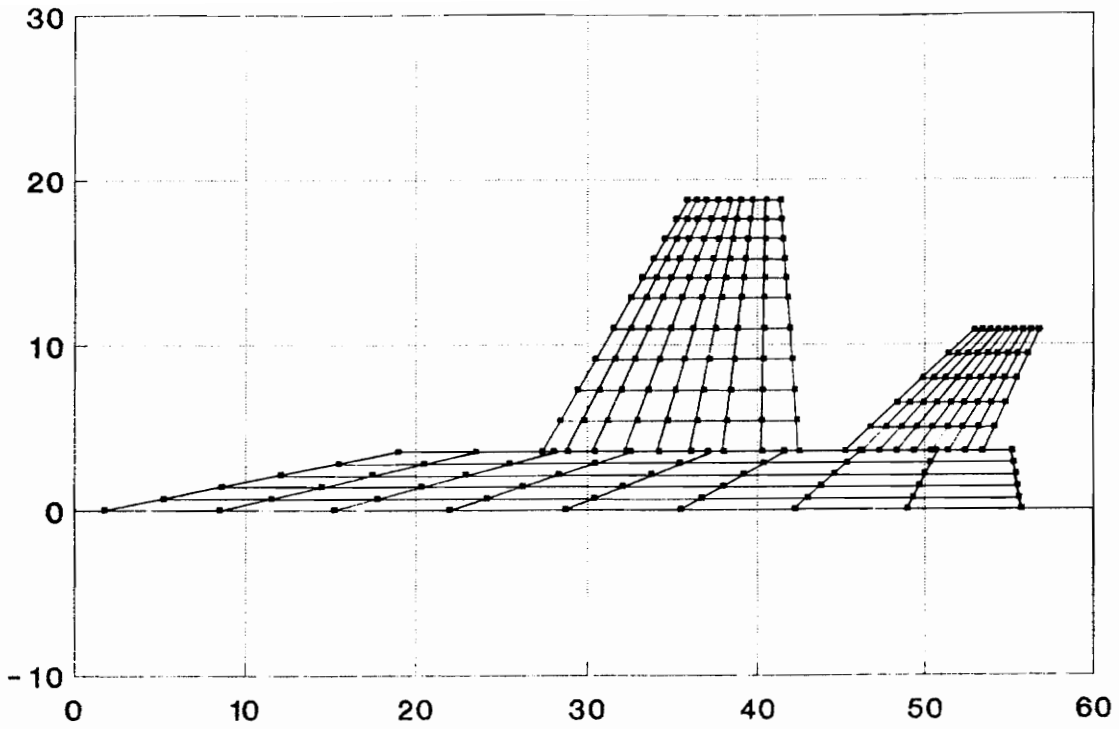


Figure 14. Vortex Rings and Corner Points of F-18 Longitudinal Planform

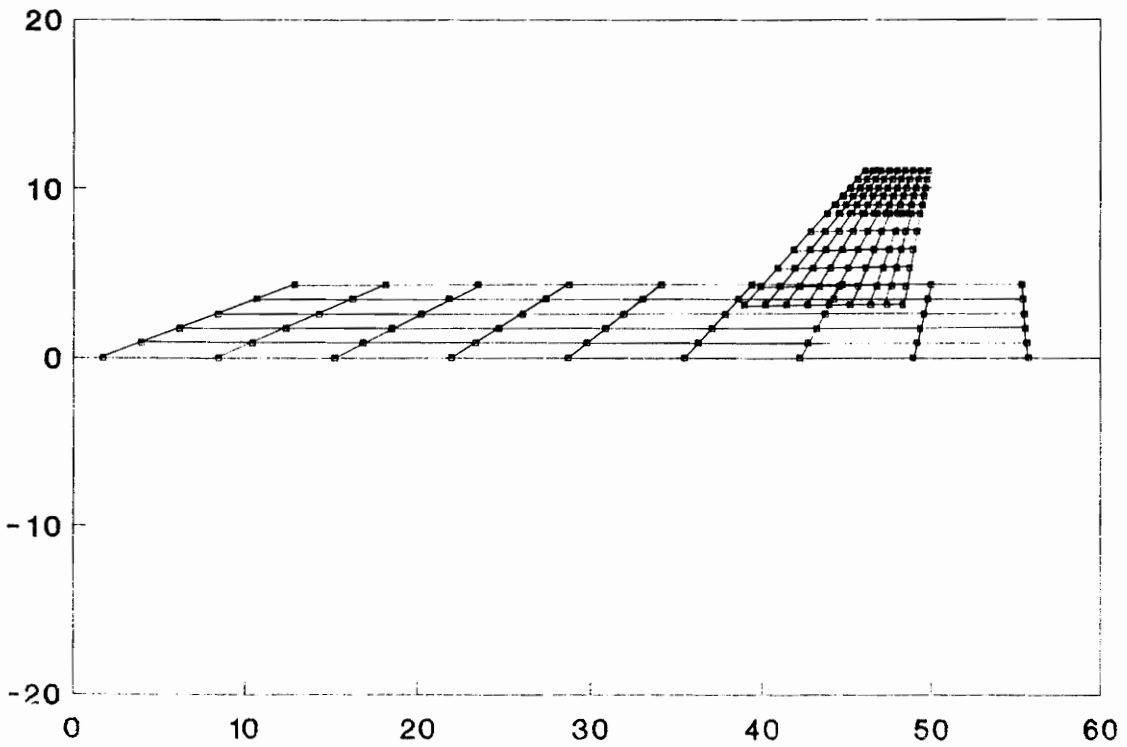


Figure 15. Vortex Rings and Corner Points of F-18 Lateral Profile

longitudinal geometry as illustrated in Figure 5. With 40 panels per section, this results in a total of 160 panels. In the lateral/directional geometry, five sections are used to represent the lateral profile of the F-18 as shown in Figure 7. Note the two vertical tails are placed on the two sides of the fuselage section. There are 200 panels representing the lateral geometry.

A complete analysis with all the output shown in Figure 8 (at one Mach number and one CG location) requires about 55 minutes on an IBM 386 compatible computer. A long time is required because there are five control surfaces in the longitudinal model and two in the lateral geometry. Most of the computing time is spent on computing the influence coefficients (the contribution of one vortex ring to the induced velocity at a control point).

4.2 Code Validation

In this section, the VLM program is used to predict the stability and control derivatives of the F-18. The results are compared to values obtained using the procedures outlined in Ref. 16, which is based on the US Air Force DATCOM. A computer program, written by Carey Buttrill of NASA Langley, that extracts stability and control derivatives from wind tunnel data was used to provide the actual F-18 result for comparison. The same data base is also used in the High

Angle-of-Attack Research Vehicle program (HARV). The comparisons are conducted at Mach 0.2 and Mach 0.6 out of ground effect, with the CG located at the quarter chord of the wing's mean chord. Note that the data and the two estimation methods all exclude aeroelastic effects.

4.2.1 Stability Derivatives

Figure 16 contains the comparison of the AOA-derivatives and the Static Margin estimates. For the lift-curve slope, the VLM and DATCOM predictions are 7% and 13% respectively lower than the wind tunnel value for Mach 0.2. The difference can partially be explained by the fact that the contribution of the twin vertical tails are ignored in both the VLM and the DATCOM estimates. Although VLM appears to have underestimated the static margin at higher Mach number, the difference is only slightly over an inch when converted to the scale of the actual aircraft, which is 56 ft long.

Figure 17 indicates that the lift-due-to-pitch rate ($C-L_q$) prediction of VLM is unacceptable. Investigation has shown that the difference is caused primarily by over-estimating the contribution from the wing. The VLM results obtained here agree with the Lamar code (Ref. 17) predictions, so that it appears that the problem is not due to an error in the VLM implementation. The exact cause of this problem is still unclear. Due to the wing's shorter moment arm to the CG, the

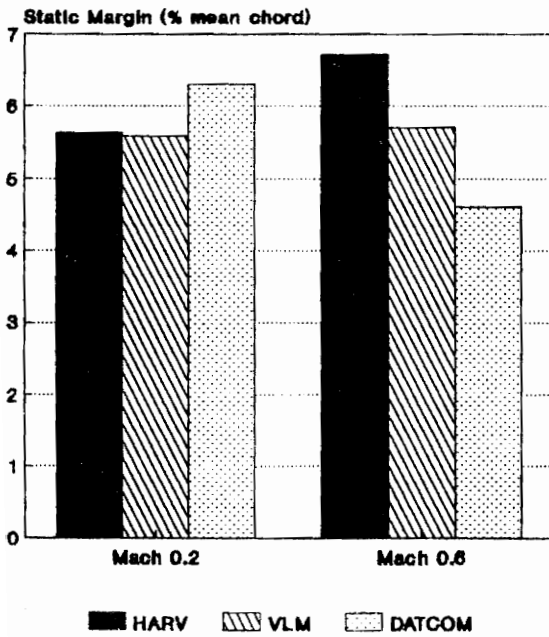
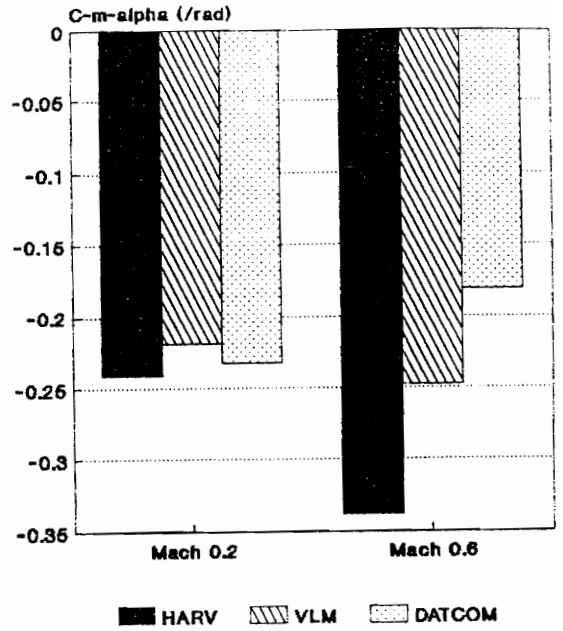
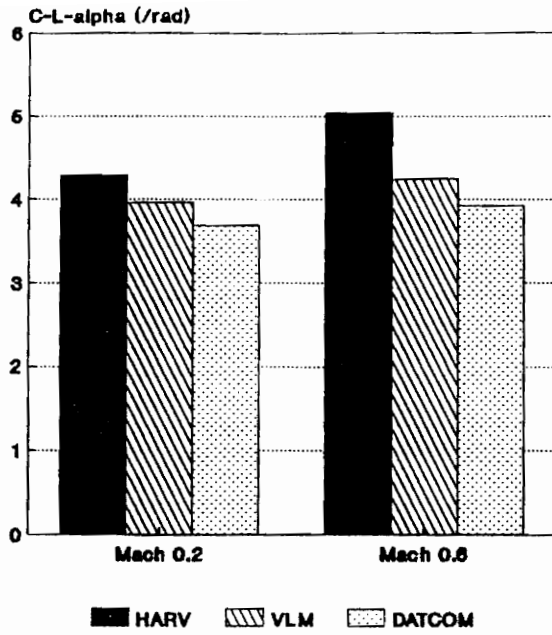


Figure 16. Angle-of-Attack Derivatives & Static Margin

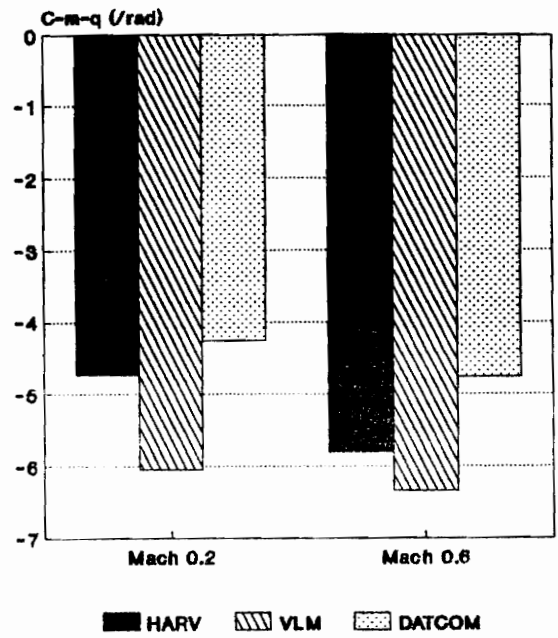
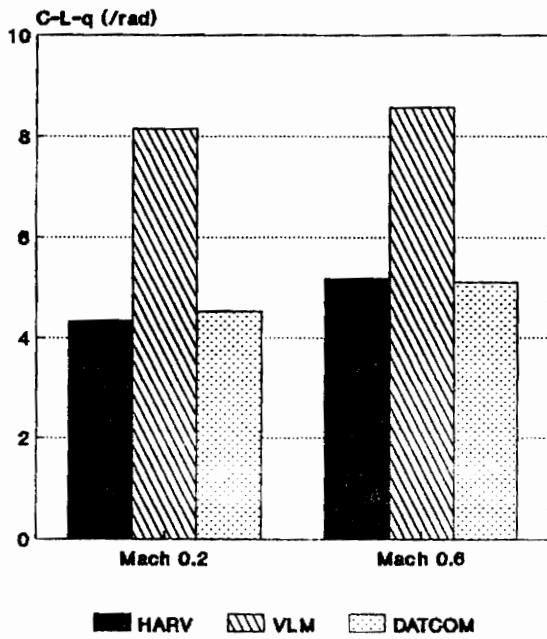


Figure 17. Pitch Rate Derivatives

influence of the over-estimation of the wing's contribution is less profound on the prediction of $C-m-q$.

Sideslip derivatives are shown in Figure 18. Both VLM and DATCOM underestimate the change in sideforce due to sideslip ($C-y-beta$) by 45 to 55%. In this case, the simplified fuselage representation (see Figure 15) is probably inadequate. The variation of roll moment due to sideslip angle ($C-l-beta$) is poorly predicted because the wing and horizontal tail are not modelled in the VLM geometry. Thus the dihedral effect is not included. The VLM's prediction of the yawing moment due to sideslip ($C-n-beta$) is within 10% of the wind tunnel value at both Mach numbers since this derivative is mostly dictated by the vertical tail(s).

The yaw-rate derivatives are shown in Figure 19. The VLM program over-predicted the sideforce variation due to yaw rate ($C-y-r$) in a manner similar to the problem with pitch rate derivative described above. Fortunately, this parameter is not used in this study. The rolling moment variation with yaw rate ($C-l-r$) is also inaccurate for the same reason. Ignoring the wing's contribution in the lateral/directional model further worsens the problem. Since the variation of yawing moment with changes in yaw rate ($C-n-r$) is generally dictated by the vertical tail volume coefficient, VLM is able to provide a prediction to within 18% of the wind tunnel value.

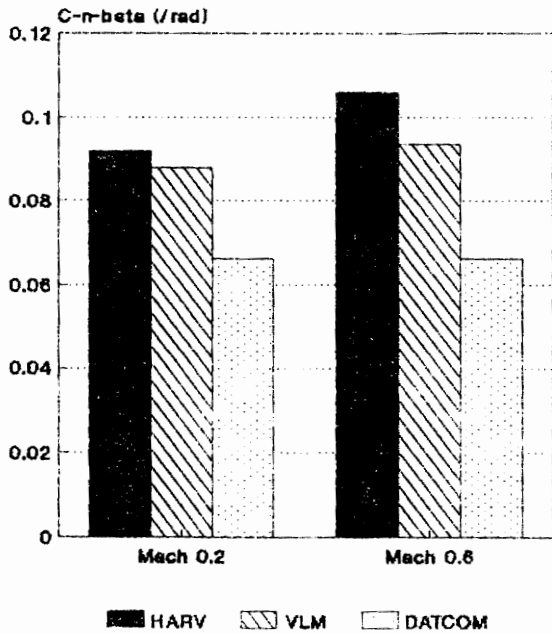
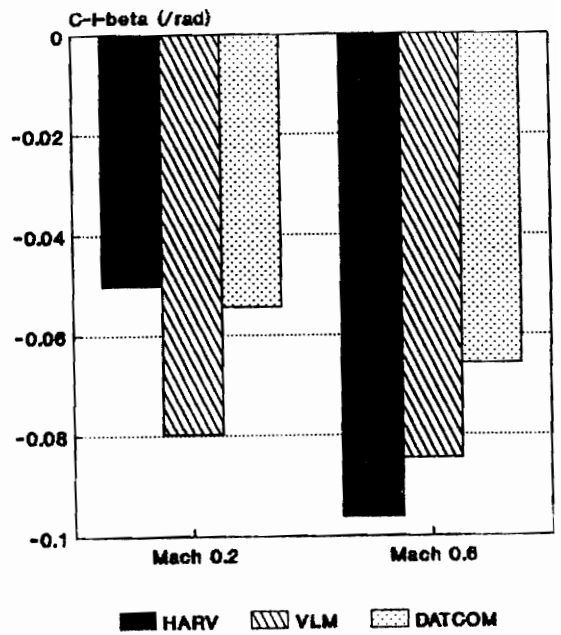
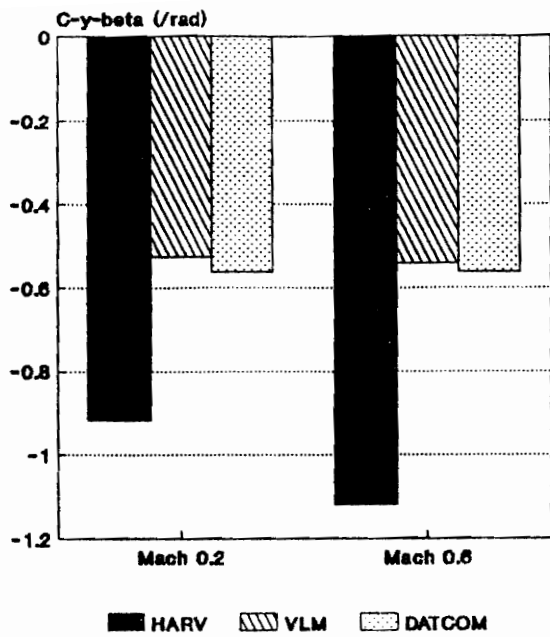


Figure 18. Sideslip Derivatives

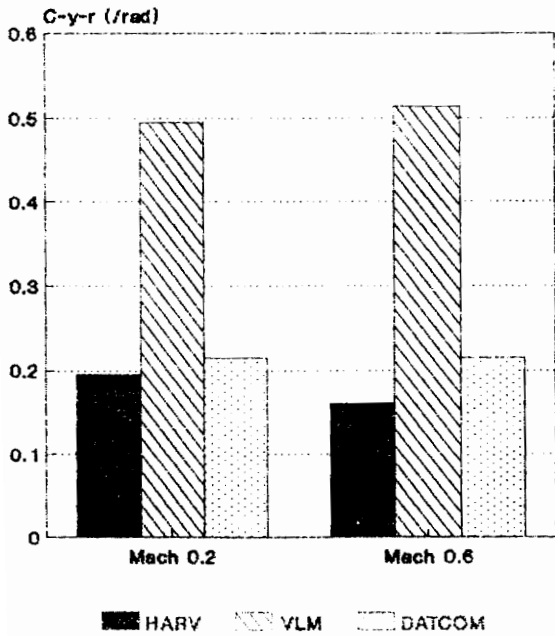
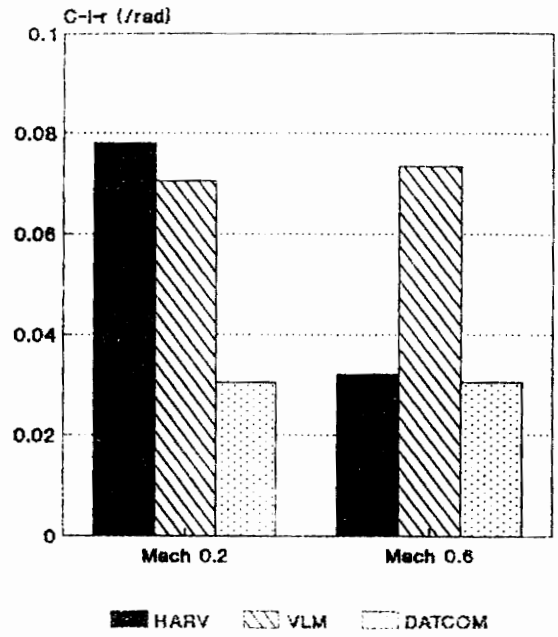
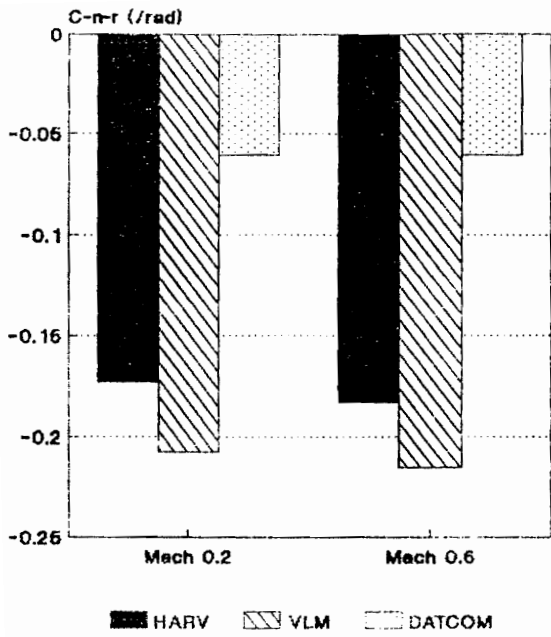


Figure 19. Yaw Rate Derivatives

The VLM approach is able to accurately predict roll rate damping coefficient (C_{l-p}) as shown in Figure 20. The slight over prediction of is caused by the poor fuselage model in both the longitudinal and lateral/directional model. The value of the yawing moment due to roll rate (C_{n-p}) is affected by 1) the dihedral of the horizontal tail, 2) the difference of the induced drag on the two sides of the wing during roll if the wing is generating net lift, and 3) the vertical tail. VLM is unable to accurately predict this stability derivative.

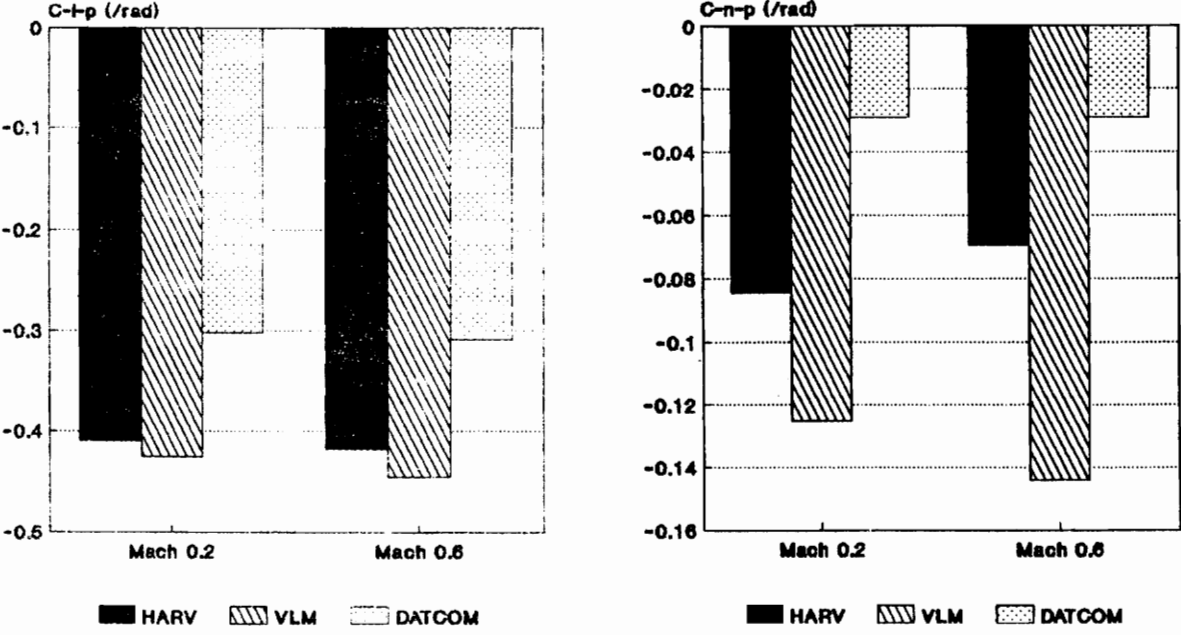


Figure 20. Roll Rate Derivative

Table 3 is the qualitative comparison the overall stability derivative estimation capability of the VLM program against DATCOM. While the VLM approach exhibits poor accuracy in certain cases (pitch and yaw rate derivatives), it appears to provide more accurate overall results than DATCOM.

Table 3. Reliability of Stability Derivative Predictions Compared to Wind Tunnel Data

	VLM	DATCOM
AOA-Derivatives	good	acceptable
q-Derivatives	deficient	good
C-y-beta & C-l-beta	deficient	deficient
C-n-beta	good	acceptable
C-y-r & C-l-r	deficient	good
C-n-r	good	deficient
p-Derivatives	good	acceptable

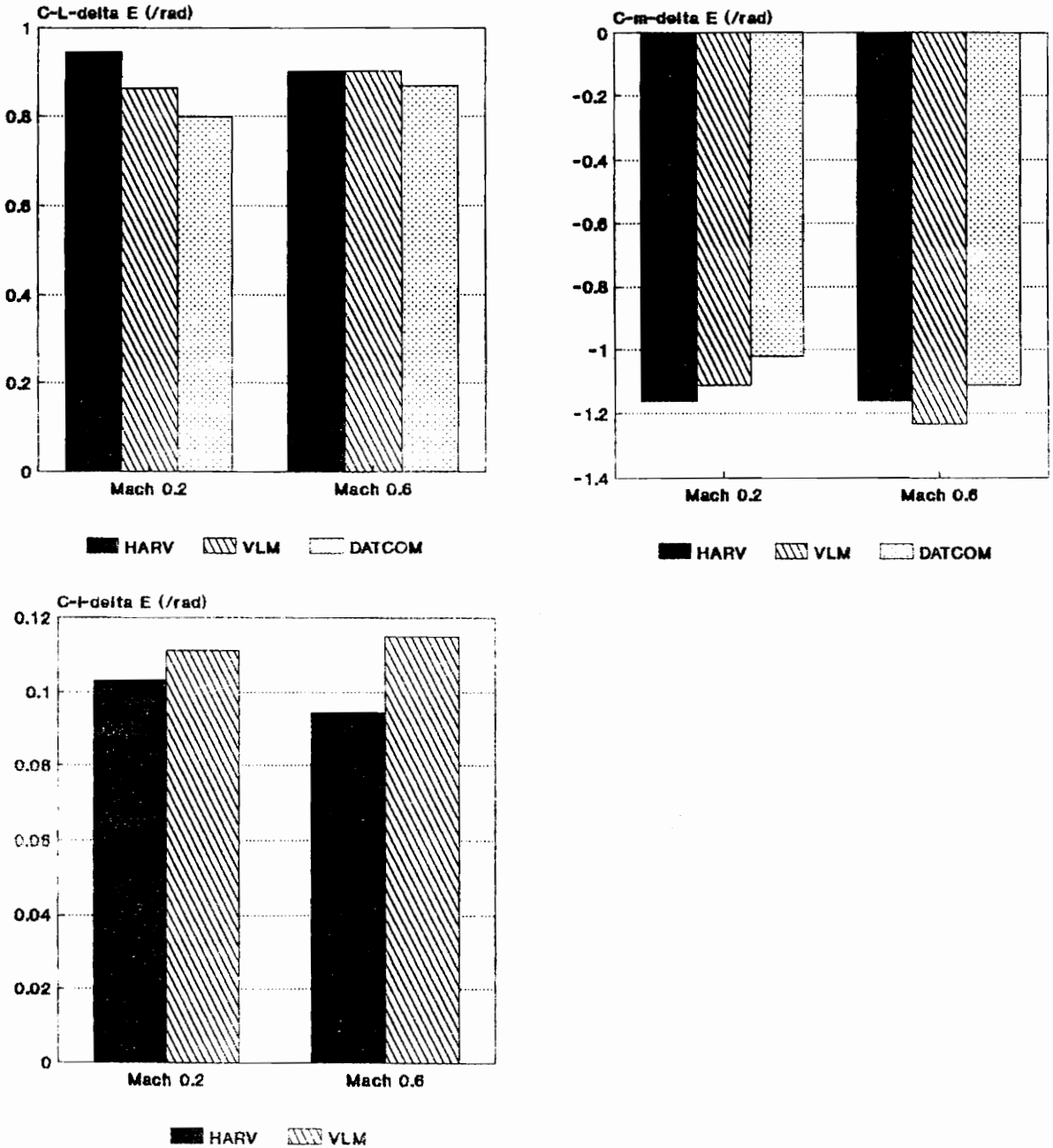
4.2.2 Control Derivatives

The HARV program generates data for control effectiveness of symmetrical control surfaces, such as flaps and elevators, on one side of the x-axis at a time. The values presented in the comparison figures are twice the magnitude of the one-side deflection values. This approximation can introduce significant error when the lateral separation between the surfaces is small as in the case of flap and elevator deflections.

Figure 21 illustrates the predictions of the elevator (horizontal tail) control effectiveness. Both VLM and DATCOM produce accurate results (VLM predictions are less than 10% from the wind tunnel values) for lift and pitching moment variations with elevator deflections ($C-L-\delta E$ & $C-m-\delta E$). In addition, VLM is able to predict the rolling moment due to antisymmetric elevator deflections. Note the loss of control effectiveness with increasing higher Mach number is evident in the HARV data. This phenomenon is observed for most control surfaces. Viscous effect may be the primary cause.

The control effectiveness of the inboard flap is shown in Figure 22. For the change of total lift and pitching moment with flap deflection ($C-L-\delta F$ and $C-m-\delta F$), the VLM result indicates good agreement with wind tunnel measurements. VLM's prediction of the rolling moment due antisymmetric flap

deflection ($C-l\text{-}\delta F$) is larger than the wind tunnel data due to the reason stated at the beginning of this section.



Antisymmetric Deflection

Figure 21. Elevator (Horizontal Tail) Effectiveness

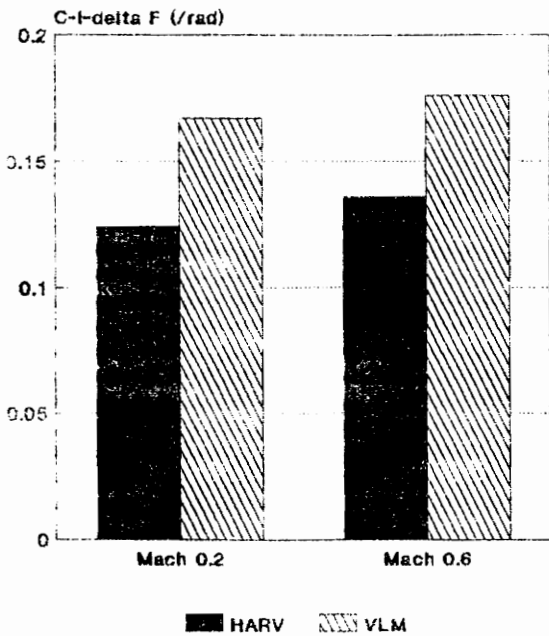
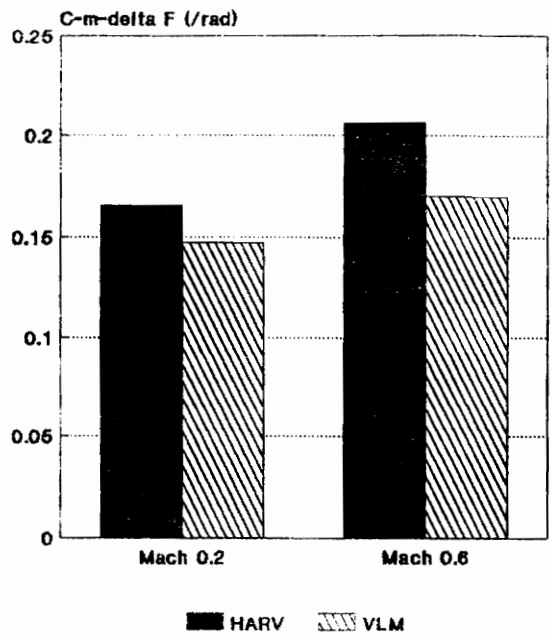
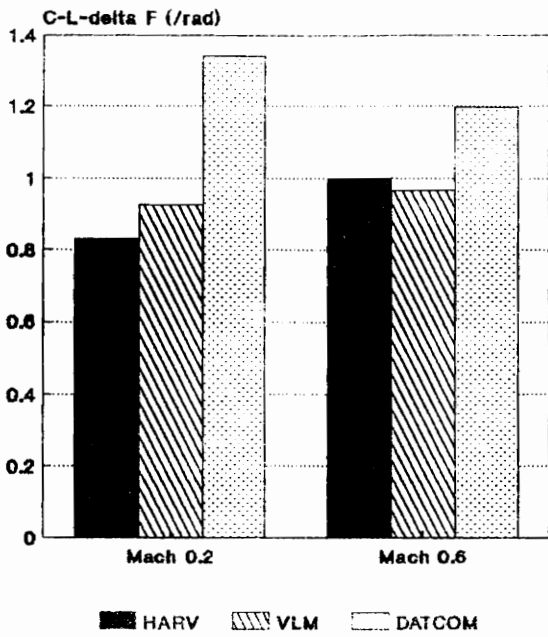


Figure 22. Inboard Trailing Edge Flap Effectiveness

The aileron roll power ($C-l-\delta A$) is shown in Figure 23. Datcom produces slightly more accurate results than the VLM approach.

The comparison of the rudder control effectiveness is shown in Figure 24. The VLM program is able to produce estimates for the sideforce and yawing moment ($C-y-\delta R$ and $C-n-\delta R$) with rudder deflection to within 15% of the wind tunnel results.

However, DATCOM produces more accurate $C-l-\delta R$.

The following two conclusions can be made about using VLM to perform control derivative estimation.

- 1). The primary control derivatives are well predicted. ie: $C-L-\delta F$, $C-m-\delta E$, and $C-l-\delta A$
- 2). Cross-coupling control derivatives that are caused mainly by change in induced drag during deflection are not well-predicted. ie: $C-n-\delta A$. Fortunately, these values usually are of less importance compared to the primary control derivatives at low AOA.
- 3). As the Mach number increases, the experimentally obtained control derivatives tend decrease in magnitude apparently due to viscous effects. Therefore when using VLM's control derivatives at higher Mach number, the users should be aware of this phenomenon.

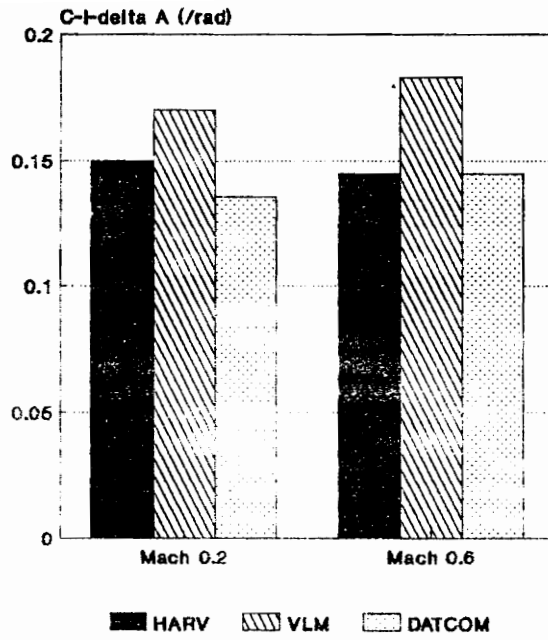


Figure 23. Aileron Effectiveness

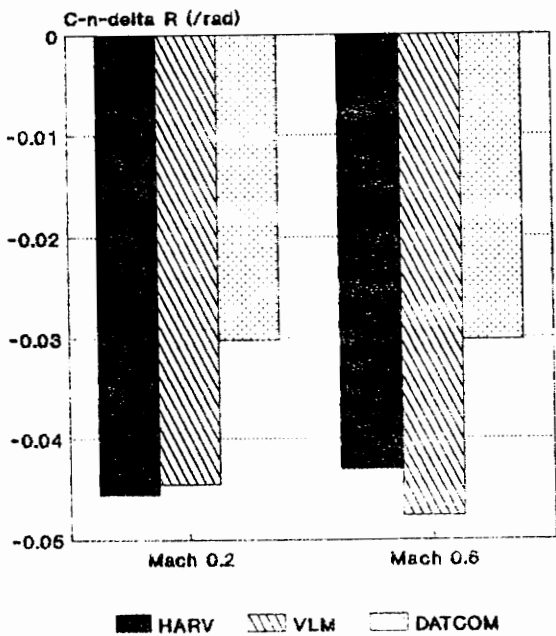
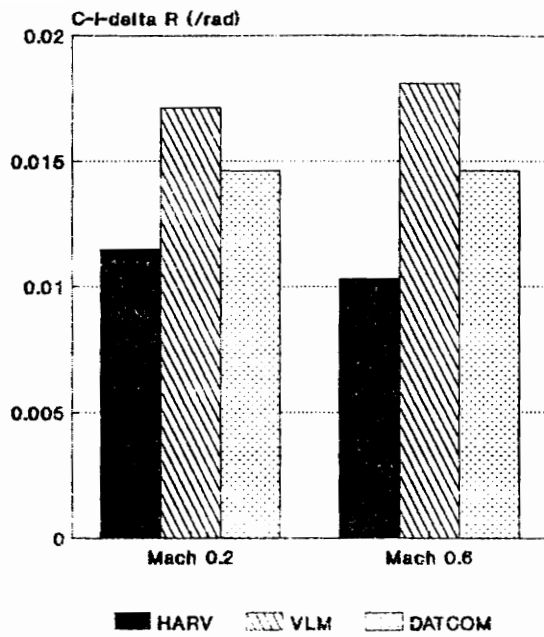
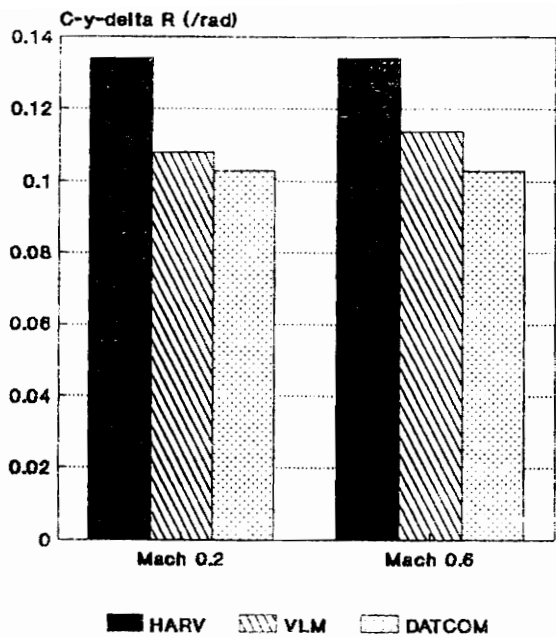


Figure 24. Rudder Effectiveness (One-Rudder Deflection)

5. Control Authority Assessment Example: The F-18

An example of the control authority assessment process is discussed in this section using the F-18's geometry and mass properties. For this study, a controller is considered saturated when it is deflected by 25 degrees.

5.1 Takeoff and Landing Rotations

Assuming the takeoff flap setting is 10 degrees, elevator trailing edge up at 25 degrees, and the tail-down angle at 15 degrees, the stall speed (assuming the maximum total lift coefficient occurs when AOA reaches the tail-down angle) with a maximum weight of 51,900 lbs is estimated to be 303 ft/sec. Note the aerodynamics properties are based on VLM's prediction in ground effect with CG at 6.5 ft above the ground. This model does not reflect the actual F-18 operation, which includes rudder toe-in to generate additional nose-up pitching moment. The results indicate that nose-up rotation can be initiated when the speed reaches 274 ft/s. A numerical integration is performed to check the speed when the tail-down angle is reached (which should occur before $0.9 V_{\min}$ according to MIL-STD-1797). Unfortunately the configuration failed to obtain the take-off attitude of 15-deg AOA prior to $0.9 V_{\min}$. Another 0.5 second past $0.9 V_{\min}$ is required before the desired AOA is reached. This simple simulation represents the worst

condition, when the aircraft is configured with its maximum weight with the CG at its most forward location.

Analysis is also performed to check whether the pitch controller has enough authority to gently lower the nose down to $0.9 V_{min}$ in landing configuration. In this case, the flap is assumed to be set at 25 degrees. The touch down speed for maximum weight is estimated at 305 ft/sec. The total moment from touch down to $0.9 V_{min}$ is positive (nose-up) for all angles of attack. Therefore it can be concluded that the configuration has enough pitch authority to meet the landing requirement.

5.2 1-G Trim

The level-flight trim capability of the pitch controller is checked under various flight conditions. The table 4 summarizes the results. The most critical condition occurs at $V = 250$ ft/sec with maximum weight and CG at its most forward location. In this case, less than 13 degrees of elevator deflection is needed. Note in this case, the required AOA is nearly 30 deg. Generally, this oversteps the realm of linear aerodynamics; and the predicted elevator deflection for trim may not be valid. Despite this problem, the configuration appears to exhibit adequate pitch control power to achieve 1-G trim.

Table 4. 1-G Trim Assessment

Weight (lbs)	S.M.	Altitude (ft)	Speed (ft/s)	AOA (deg)	Elevator (deg)
51900	13.3%	0	250	28.7	-12.4
51900	13.3%	0	1695	0.58	-.93
38400	5.4%	50,000	600	20.5	-2.98
38400	5.4%	50,000	1030	3.23	-3.87

Table 5. Maneuver Flight (Pull-up) Assessment

Weight (lbs)	S.M.	Alt. (ft)	Speed (ft/s)	G's	AOA (deg)	Elev. (deg)
51900	13.3	0	250	1.5	42.2	-19.1
51900	13.3	0	1695	9	4.35	-2.0
38400	5.4	50,000	553	1.5	34.4	-6.35
38400	5.4	50,000	1745	9	24.6	-33.9

5.3 Maneuver Flight (Pull-up)

Table 5 summarizes the tests performed to check the pitch controller's effectiveness to satisfy the pull-up requirements. There may not be enough elevator power to generate the maximum load factor of 9-G's at the maximum speed at 50,000 ft. However, obtaining 9-G's near the ceiling is not likely to be an important issue.

5.4 Short Period & CAP Requirements

Short period & Control Anticipation Parameter tests are performed at different potentially critical flight conditions (Table 6). All but the Mach 1.2 case satisfy the level-1 flying quality requirements. Inadequate damping resulting in a level-2 condition is observed at Mach 1.2. at 10,000 ft. However, the deficiency appears to be small enough to allow the augmented flight control systems to correct the problem.

5.5 Pitch Due to Velocity Axis Roll

The test of pitch authority to counter velocity-axis roll is performed at Mach .6 at sea level. Assuming 60% of the total pitch effectiveness can be allocated to coping with the pitch-up tendency, a plot of maximum stability-axis roll rate vs. angle of attack can be obtained (Figure 25). Depending on the performance requirement, the designer can decide whether the pitch controller will become a limiting factor in the

Table 6. Short Period & Control Anticipation Parameter (CAP) Assessment

Weight	S.M.	Alt	Mach	Natural Frequency	Damping Ratio	CAP
(lbs)	% c	(ft)		(rad/s)		(1/g/s ²)
50000	13.2	0	0.2	0.78	0.42	0.256
24800	13.2	0	0.2	0.98	0.57	0.202
36000	5.4	10,000	0.8	3.48	0.40	0.286
36000	5.4	10,000	1.2	10.06	0.22	1.061

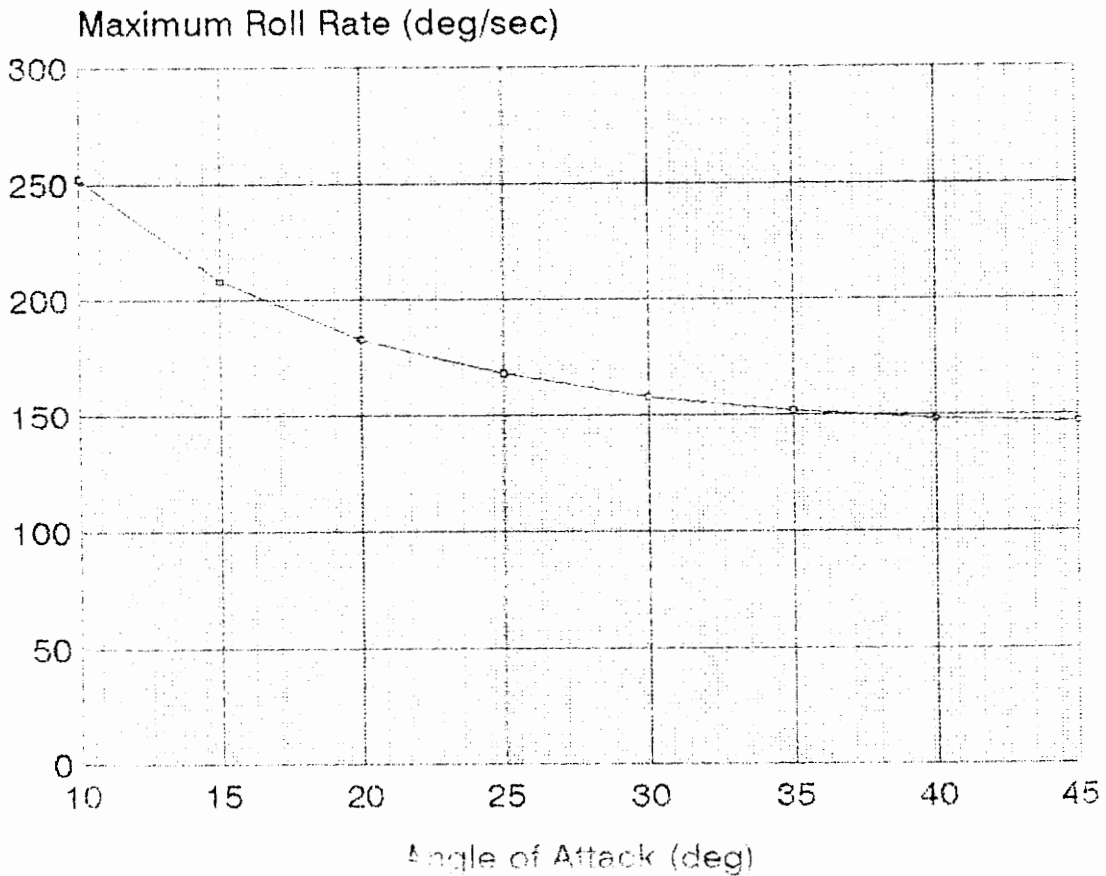


Figure 25. Estimated Maximum Stability Axis Roll Rate of F-18 Limited by Elevator Power, @ SL, Mach 0.6

configuration's stability-axis roll capability.

5.6 Steady Sideslip

The aircraft's ability to maintain sideslip at very low speed is tested. To achieve 30 degrees of sideslip, the rudder must be deflected 24.9 degrees. Allowing a 25% yaw control margin as prescribed by MIL-STD-1797, a steady sideslip angle of 18.5 degrees can be achieved in the test case. Therefore the configuration is expected to have enough control authority to land in a 30-knot cross-wind with a landing speed as low as 95 knots.

5.7 Engine-out Trim

The yaw and roll controllers' effectiveness are tested against adverse yaw conditions as a result of asymmetric loss of thrust. In this case, 15,000 lbs thrust is assumed to be generated by the right engine. Note that this asymmetric thrust is chosen near the maximum thrust of one engine to account for the additional drag because of possible sideslip and the asymmetric drag created by the failed engine. The results are shown in Table 7. Depending on the weight of the aircraft, there is sufficient rudder power to create -3.5 to +4.5 degrees of bank angle while complying with the requirement that no more than 75% of the yaw and roll effectiveness be used to cope with asymmetric thrust.

Table 7. Engine-out Trim Assessment at Mach 0.2 at SL

Weight (lbs)	Bank Angle (deg)	Sideslip (deg)	Aileron (deg)	Rudder (deg)
30,000	+4.5	+10.8	+6.9	+10.1
30,000	0.0	-3.3	+2.9	-3.3
30,000	-2.0	-9.5	+1.1	-9.2
30,000	-4.5	-18.0	-1.3	-17.2
40,000	+4.5	+15.5	+8.2	+14.5
40,000	0.0	-3.3	+2.9	-3.3
40,000	-3.5	-17.1	-1.3	-17.1

5.8 Time-to-Bank

The roll performance of the F-18 is assessed against the general time-to-bank requirement of table 1b. Table 8 summarizes the time required to roll through the specified angles along with the speed at which the configuration is tested. When compared to the requirements in Table 1b, the F-18 demonstrates superior roll capability.

5.9 Rolling Pullout & Coordinated Roll

To assess the configuration's yaw and roll control effectiveness, an analysis was performed at Mach .6 at sea level. Different combinations of roll rate, roll acceleration and normal load factors were applied. Table 9 indicates that most coordinated roll performance of the F-18 appears to be limited mainly by the lack of yaw control authority.

5.10 Overall Assessment

The F-18 appears to lack elevator power to obtain the take-off attitude during the takeoff roll with maximum weight and the CG at its most forward location. This problem alone does not warrant increasing the horizontal tail volume. A possible alternative is to decrease the tip-back angle by moving the main gear forward. The rudder power appears to be the marginally adequate while there appears to be sufficient

roll authority.

Table 8. Time-to-Bank Performance at SL (Ix = 26000 slug ft²)

	Speed	30 deg	90 deg	180 deg	360 deg.
	(ft/sec)	(sec)	(sec)	(sec)	(sec)
VL	334	0.58			
L	368		0.91	1.40	2.25
M	468		0.73	1.10	1.77
H	1186		0.40	0.65	1.15

Table 9. Rolling Pullout & Coordinated Roll Assessment at SL, Mach 0.6

P_{stab} (deg/s)	$P\text{-Dot}_{stab}$ (deg/s ²)	Load Factor (G)	AOA (deg)	Rudder (deg)	Aileron (deg)
180	0	0.0	0.0	-4.9	+12.5
180	0	2.0	3.1	-8.0	+13.0
180	0	4.0	6.3	-12.2	+13.5
360	0	0.0	0.0	-9.8	+25.0
360	0	2.0	3.1	-17.0	+26.1
0	180	5.0	45.0	-27.1	+7.5
0	360	5.0	18.0	-24.0	+10.7
180	180	5.0	28.0	-23.5	+16.1

6. Conclusion

In this study, a methodology that allows aircraft designers to quickly assess candidate concepts against the control authority requirements early in the design phase was established. Flight conditions and maneuvers that result in great demands on control power were identified. A vortex lattice method program was written to speed up the process of estimating the design's stability and control derivatives for subsonic, low angle-of-attack flight regimes. Finally, a spreadsheet was created to apply the estimated stability and control derivatives to the dynamics equations to check whether the configuration possesses sufficient control power. Applying this methodology should ensure that the conceptual design team can identify deficient control power early in the preliminary design stage, when design modifications can be made without major complications.

6.1 Future Work

Although this study has identified many critical maneuvers and flight conditions that are known to deplete available control authority, future super agile aircraft with frequent excursions into the high angle-of-attack regime are likely to demand even more control authority. To assure stability and controllability at high AOA, the designers will

need to be able to evaluate the configurations' aerodynamic characteristics at high AOA.

To improve the accuracy of the stability and control derivative estimates for subsonic, low-AOA flights, a more sophisticated vortex lattice method with more efficient use of panels should be explored. A better fuselage representation could further enhance accuracy of the stability and control derivative estimates. In addition, effects of aeroelasticity and viscosity should be approximated using empirical correlation approach. If sufficient reliability can be achieved, the control authority assessment process can even be incorporated as part of the design optimization cycle.

Furthermore, the possibility of using thrust vectoring to augment the longitudinal and lateral/directional controllers introduces a new dimension to the problem in which because of the redundant controllers, issues such as control power allocation should be considered in the conceptual design stage.

References:

1. Hoak, D. E.; Ellison, D. E. et al.; USAF Stability and Control DATCOM; Flight Control Division; Air Force Flight Dynamics Laboratory, Wright Patterson Air Force Base, Ohio.
2. MIL-W-25140 Weight and Balance Control Data for Airplanes and Rotorcraft.
3. Roskam, Jan. *Airplane Design Part V Component Weight Estimation*. Roskam Aviation and Engineering Corporation. Ottawa, Kansas. 1988.
4. MIL-STD-1797. *Flying Qualities of Piloted Vehicle*. 1987.
5. Roskam, J. *Airplane Design. Part VII: Determination of Stability, Control and Performance Characteristics: FAR and Military Requirements*. Roskam Aviation and Engineering Corporation, Kansas, 1988.
6. Etkin, B. *Dynamics of Atmospheric Flight*. John Wiley & Sons, Inc., New York 1972.
7. Nelson, R. C. *Flight Stability and Automatic Control*. McGraw-Hill Co, New York 1989.
8. Chody, J. R., Hodgkinson, J. and Skow, A. M. "Combat Aircraft Control Requirements for Agility." AGARD CP-465, Oct. 1989.

9. Nguyen, L. T., Ogburn, M. E., Gilbert, W. P., Kibler, K. S., Brown, P. W., and Deal, P. L. "Simulator Study of Stall/Post-Stall Characteristics of a Fighter Airplane with Relaxed Longitudinal Static Stability." NASA TP-1538, NASA-Langley, Dec. 1979.
10. Mercadante, R. "Basic Agility/Control Power Requirements for Advanced Supersonic Fighter Configurations." Grumman Memorandum, EG-ARDYN-83-82. Oct. 1983.
11. Lutze, F. H., Durham, W. C., and Mason, W. H. "Development of Lateral-Directional Departure Criteria." Final Report for NASA/LRC Project NCC1-158. Dept. of Aerospace & Ocean Engineering, VPI & SU. June, 1992.
12. Johnston, D. E. and Heffley, R. K. "Investigation of High AOA Flying Quality Criteria & Design Guides." AFWAL-TR-81-3108, December 1981.
13. Bihrlé, W., Jr. and Barnhart, B. "Departure Susceptibility and Uncoordinated Roll-Reversal Boundaries for Fighter Configurations." AIAA Journal of Aircraft, Vol. 19, No. 11, Nov. 1982, P. 897.
14. Bertin, J. and Smith, M. Aerodynamics for Engineers. 2nd ed. Prentice Hall, New Jersey 1989.
15. Katz, J. and Plotkin, A. Low-Speed Aerodynamics: From Wing Theory to Panel Methods. McGraw-Hill, Inc. New York 1991.
16. Roskam, J. Methods for Estimating Stability and Control Derivatives of Conventional Subsonic Airplanes. Roskam

Aviation and Engineering Corporation, Kansas 1971.

17. Lamar, J. E. and Gloss, B. B. "Subsonic Aerodynamics Characteristics of Interacting Lifting Surface with Separate Flow Around Sharp Edges Predicted by a Vortex-Lattice Method." NASA TN D-7921, Sept., 1975

Appendix A. Program and Spreadsheet Documentation

A1. VLM Program

The vortex lattice method (VLM) program developed in this study was written in Microsoft FORTRAN to be used on IBM compatible PCs. The program's major subroutines and their functions are:

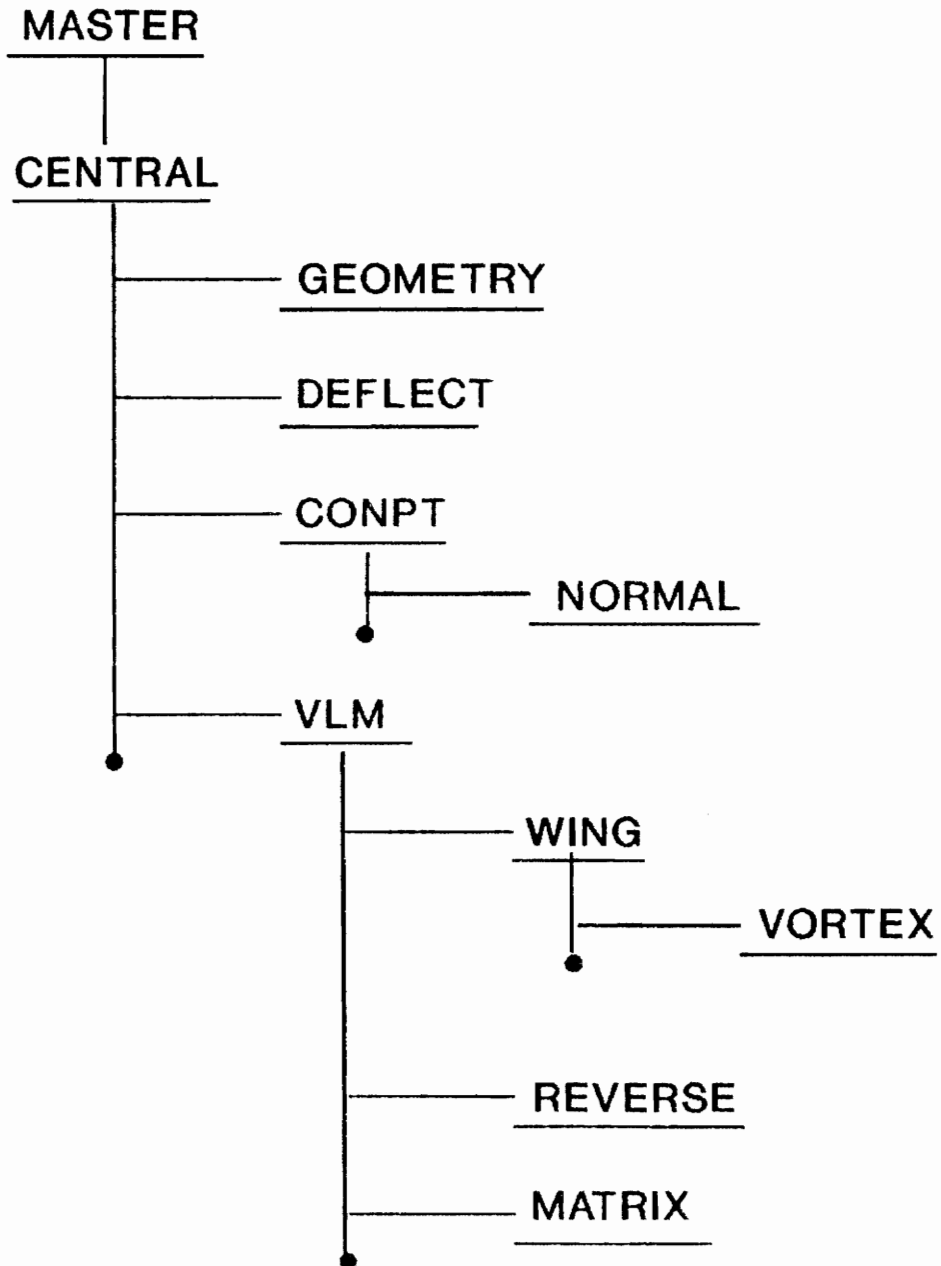
Prgrm/Subrtn	Functions
MASTER	User interface. Controls variation in flow. (control deflection, AOA, etc.) Calls CENTRAL. Performs finite difference on forces & moments. Stab. & control derivatives output.
CENTRAL	Reads GEOMETRY & LATGEOM for corner points. Calls GEOMETRY; DEFLECT; CONPT; VLM.
GEOMETRY	Determines corner pts of vortex rings.
DEFLECT	Rotates corner points about the hinge line in 3-D.
CONPT	Determines control point locations. Calls NORMAL.
NORMAL	Determines panels' normal vectors & areas.

VLM	<p>Calls WING to calc. Influence Coefficient.</p> <p>Calls REVERSE to reverse surface deflection for asymmetric deflection.</p> <p>Calls MATRIX to solve for vortex strengths.</p> <p>Calculates Forces and Moments.</p>
WING	<p>Determines the induced velocity at control points by a vortex ring.</p> <p>Calls VORTEX.</p>
VORTEX	<p>Uses Biot-Savart Law to find induced velocity at a point by a vortex segment.</p>
MATRIX	<p>Solves a system of linear equations.</p>
REVERSE	<p>Reverses control surface's deflection for antisymmetric deflection cases.</p>

The connection between the VLM's subroutines is illustrated in the following page.

Note in the output, positive control deflection is TE down and LE up for longitudinal controls and TE right for directional controls. In addition, the lift-curve slope of H tail due to the downwash of wing is also available to be used to determine $C_m\text{-}\alpha\text{-dot}$.

VLM Program's Subroutines



A2. Spreadsheet to Check Control Authority Requirements

A Lotus-123 worksheet was created to check if the design configuration is able to meet the control authority requirements. It contains items discussed in section 2.1 through 2.10. The following is the sample worksheet.

Nose-wheel Lift-off

Input: Max Takeoff Gross Weight (lbs) 51900
 Max Takeoff Thrust (lbs) 33700
 Thrust Incident Angle (rad) 0
 Reference Area (ft²) 400
 Reference Chord (ft) 11.52
 Horiz. Dist. CG to main gear axle (ft) 4.2
 Vert. Dist. CG to main gear axle (ft) 5.4
 Horiz. Dist. CG to engine nozzle (ft) 20
 Vert. Dist. CG to engine nozzle (ft) -0.55
 Rolling Coefficient: tire & runway surface 0.025
 Total C-m with deflected flaps & pitch controllers 0.585
 Total C-L with deflected flaps & pitch controllers -0.222
 Air Density (slug/ft³) 0.002376
 Zero-lift Drag Coef. CD0 0.02
 CDi/CL² 0.055

Calc. Dynamic Pressure to Start Rotation. (lbs/ft²) 89.34463
 Moment Arm (ft) 6.841052
 Tip-Back Angle (rad) 0.661043

Output: Speed for Rotation (ft/sec) 274.2369
 Speed for Rotation (knots) 162.4854

 Integration to check pitch attitude at .9 V-min

Time Increment (s) 0.1
 I-y about CG (slug ft²) 140000

V (ft/s)	AOA(rad)	C-L	C-D	C-m	Dyn Press	AOA''	AOA-dot
274.2369	0	-0.222	0.022710	0.585	89.34463	-6.0E-17	0
276.4709	0	-0.222	0.022710	0.585	90.80619	0.024123	0.001206
278.7059	0.000120	-0.22135	0.022695	0.584867	92.28030	0.049183	0.004871
280.9419	0.000607	-0.21877	0.022632	0.584332	93.76691	0.076694	0.011165
283.1786	0.001724	-0.21284	0.022491	0.583106	95.26588	0.108310	0.020415
285.4156	0.003765	-0.20200	0.022244	0.580865	96.77695	0.145900	0.033126
287.6523	0.007078	-0.18441	0.021870	0.577227	98.29968	0.191625	0.050002
289.8878	0.012078	-0.15786	0.021370	0.571737	99.83350	0.247986	0.071983
292.1210	0.019277	-0.11963	0.020787	0.563833	101.3776	0.317847	0.100274
294.3508	0.029304	-0.06639	0.020242	0.552823	102.9311	0.404356	0.136385
296.5756	0.042943	0.006027	0.020001	0.537848	104.4930	0.510718	0.182138
298.7943	0.061156	0.102743	0.020580	0.517849	106.0623	0.639656	0.239657
301.0059	0.085122	0.230001	0.022909	0.491535	107.6382	0.792345	0.311257
303.2111	0.116248	0.395279	0.028593	0.457359	109.2211	0.966473	0.399198
305.4129	0.156168	0.607253	0.040281	0.413527	110.8131	1.152945	0.505169
307.6197	0.206685	0.875499	0.062157	0.358059	112.4203	1.330722	0.629352
309.8482	0.269620	1.209685	0.100483	0.288956	114.0550	1.459638	0.768871
312.1288	0.346507	1.617955	0.163977	0.204534	115.7402	1.472387	0.915472
314.5130	0.438054	2.104071	0.263491	0.104015	117.5151	1.270153	1.052599
317.0797	0.543314	2.663002	0.410036	-0.01155	119.4410	0.731810	1.152697
319.9410	0.658584	3.275084	0.609939	-0.13812	121.6064	-0.24868	1.176854

 Nose-down Rotation During Landing Rollout

Input: Max Landing Weight (lbs) 51900
 Landing Thrust (lbs) 12000
 Thrust Incident Angle (rad) 0
 Reference Area (ft²) 400
 Reference Chord (ft) 11.52
 Horiz. Dist. CG to main gear axle (ft) 4.2
 Vert. Dist. CG to main gear axle (ft) 5.4
 Horiz. Dist. CG to engine nozzle (ft) 20
 Vert. Dist. CG to engine nozzle (ft) -0.55
 Rolling Coefficient: tire & runway surface 0.025
 Air Density (slug/ft³) 0.002376
 I-y about CG (slug ft²) 140000

 Zero-lift Drag Coef. CD0 0.02
 CDi/CL² 0.055
 Tip-Back Angle (rad) 0.661043
 Moment Arm (ft) 6.841052

Check for Nose-up Moment from T.D. to 0.9 V-min

V (ft/s)	Dyn Press	AOA (rad)	C-L	C-D	C-m	Pitch M	q-dot
305	110.5137	0.262	1.42262	0.131311	0.291024	194491.0	1.389221
305	110.5137	0.1	0.5624	0.037396	0.4689	147585.5	1.054182
305	110.5137	0	0.0314	0.020054	0.5787	82332.01	0.588085
277	91.15405	0.262	1.42262	0.131311	0.291024	137510.8	0.982220
277	91.15405	0.1	0.5624	0.037396	0.4689	89272.26	0.637659
277	91.15405	0	0.0314	0.020054	0.5787	29652.53	0.211803

```

*****
Trimmed 1-G Flight
*****
Input:  Weight (lbs)                51900
        Reference Area (ft^2)       400
        Speed (ft/s)                250
        Air Density (slug/ft^3)     0.002376
        C-m-0                        0.0181
        C-m-delta E (/rad)          -1.117
        C-L-0                        -0.0685
        C-L-delta E (/rad)          0.8688
        C-m / C-L (-Static Margin)  -0.13
        C-L-alpha (/rad)            4

Output: C-L Required for 1-g trim    1.747474
        Elevator Deflection for Trim (deg) -12.4386
        AOA Required for 1-g Trim (deg) 28.71360

```

```

*****
Maneuver Flight (Pull-up)
*****

Input:  Weight (lbs)                51900
        Reference Area (ft^2)       400
        Reference Chord (ft)        11.52
        Speed (ft/s)                1695
        Air Density (slug/ft^3)     0.002376
        Dynamic Pressure (lbf/ft^2) 3413.153

        C-m-0                        0
        C-m-delta E (/rad)          -1.06
        C-L-0                        0
        C-L-delta E (/rad)          0.65
        C-m / C-L (-Static Margin)  -0.35
        C-L-alpha (/rad)            5.57
        C-m-q (rad)                 -6.22
        C-L-q (rad)                 5.51
        Load Factor. (g)             9

Calc.   C-L Required for 1-g trim    0.038014
        Elevator Deflection for 1-g Trim (rad) -0.01598
        AOA for 1-g Trim (rad)       0.008689

        RHS1:                        0.292734
        RHS2:                        0.003212

        [A]:                          5.57    0.65
                                   -1.9495   -1.06

        [A]^-1:                       0.228594 0.140176
                                   --0.42042 -1.20120

Macro:  /dmig160.h161~g163.h164~/dmmg163.h164~h157.h158~h168.h169~

Output: Delta-alpha (rad)            0.067368
        Delta-delta E (rad)         -0.12693

        Total AOA required (deg)     4.357800
        Total Elevator Deflection (deg) -8.18828

NOTE:   Press <ALT-M> to recalculate

```

```

*****
Short Period & Control Anticipation Parameter (CAP)
*****
Input:  Weight (lbs)                34297
        I-y (slug ft^2)            123936
        Reference Area (ft^2)      400
        Reference Chord (ft)       11.52
        Speed (ft/s)               1291
        Density (slug/ft^3)        0.001755
        Dynamic Pressure, q (lbf/ft^2) 1462.512
        C-L-alpha (/rad)           5.6
        C-m-alpha (/rad)           -1.79
        C-m-q (/rad)               -6.86
        C-m-alpha-dot (/rad)       -1.5

Output: Natural Frequency (/s)      10.06478
        Damping Ratio               0.219113
        N-alpha (G/rad)             95.51937
        Control Anticipation Parameter, CAP (rad/sec^2/g) 1.060515
        Control Anticipation Parameter, CAP (deg/sec^2/g) 60.76307

```

Pitch Due to Roll Inertial Coupling

Input:	Weight (lbs)	500
	I-x (slug ft ²)	23168
	I-y (slug ft ²)	123936
	I-z (slug ft ²)	143239
	Reference Area (ft ²)	400
	Reference Chord (ft)	11.52
	Density (slug/ft ³)	0.002376
	Speed (ft/s)	670
	Velocity Axis Roll Rate (deg/sec)	147
	Angle of Attack (deg)	60
	C-m-delta-E (/rad)	-1.23
Output:	Dynamic Pressure, q (lbf/ft ²)	533.2932
	Pitch Moment Coeff. due to Roll Coupling (+ or -)	0.278534
	Additional Elev. Deflection to Counter Coupling (rad)	0.226451
	Additional Elev. Deflection to Counter Coupling (deg)	12.97469

 Engine-out Trim (Aileron & Rudder Deflections)

Input:	C-l-beta (/rad)	-0.0803
	C-n-beta (/rad)	0.0868
	C-Y-beta (/rad)	-0.532
	C-l-delta-Aileron (/rad)	0.171
	C-n-delta-Aileron (/rad)	-0.0046
	C-Y-delta-Aileron (/rad)	0
	C-l-delta-rudder (/rad)	0.033
	C-n-delta-rudder (/rad)	-0.09
	C-Y-delta-rudder (/rad)	0.22
	Thrust Difference (lbf)	15000
	Engine Nozzle's X-dist. from CG (ft)	21
	Engine Nozzle's Y-dist. from CG (ft)	1.5
	Vertical Nozzle Deflection (deg)	0
	Horizontal Nozzle Deflection (deg)	2
	Speed (ft/sec)	250
	Air Density (slug/ft^3)	0.002376
	Weight (lbs)	40000
	Reference Area (ft^2)	400
	Reference Span (ft)	34.72
	Dynamic Pressure (lbf/ft^2)	74.25
	Bank Angle (deg)	-3
Calc:	C-Y-delta-Thrust	-0.01762
	C-n-delta-Thrust	-0.01114
	C-l-delta-Thrust	0
	RHS1	0.088112
	RHS2	0.011145
	RHS3	0
	Matrix A:	-0.532 0.22 0
		-0.0803 0.033 0.171
		0.0868 -0.09 -0.0046
	Inverse A:	-3.09557 -0.20558 -7.64234
		-2.94021 -0.49713 -18.4805
		-0.88624 5.847352 -0.02234
Macros:	/dmid355.f357~d359~/dmmd359.f361~h351.h353~h366~	
Note:	Hit <ALT-I> to Recalculate	
Output:	Sideslip Angle (rad)	-0.27504
	Rudder Deflection (rad)	-0.26460
	Aileron Deflection (rad)	-0.01291
	Sideslip Angle (deg)	-15.7591
	Rudder Deflection (deg)	-15.1610
	Aileron Deflection (deg)	-0.74013

 Steady Sideslip Flights (Aileron & Rudder Deflections)

Input:	Sideslip Angle, beta, (deg)	18.5
	Sideslip Angle, beta, (rad)	0.322885
	C-l-beta (/rad)	-0.05025
	C-n-beta (/rad)	0.09169
	C-l-delta-Aileron (/rad)	0.171
	C-n-delta-Aileron (/rad)	-0.0045
	C-l-delta-rudder (/rad)	0.0337
	C-n-delta-rudder (/rad)	-0.08988
Output:	Aileron Deflection (rad)	0.030267
	Aileron Deflection (deg)	1.734187
	Rudder Deflection (rad)	0.327872
	Rudder Deflection (deg)	18.78572

 Time-to-Bank Performance

Input: I-x (slug ft²) 26000
 Reference Area (ft²) 400
 Reference Span (ft²) 34.72
 Air Density (slug/ft³) 0.002376
 Speed (ft/sec) 334

Max Aileron Deflection Rate (rad/sec) 3.1
 Max Aileron Deflection Angle (rad) 0.436
 C-l-delta-Aileron (/rad) 0.17
 C-l-p. roll rate damping (/rad) -0.4239
 Integration Time Step (sec) 0.05

Output: Dynamic Pressure (lbf/ft²) 132.5285
 L-delta-Aileron (lbf-ft/rad) 312894.5
 L-p (lbf-ft/rad) -40552.3
 Time to Max Aileron Deflection (sec) 0.140645

 Integration to Check Roll Performance:

Time (sec)	Delta-A (rad)	Delta-A (deg)	L-total (lbf-ft)	p-dot (rad/s ²)	p (rad/sec)	Bank Angle (rad)	Bank Angle (deg)
0	0	0	0	0	0	0	0
0.05	0.155	8.880845	48498.65	1.865332	0.046633	0.001165	0.066797
0.1	0.31	17.76169	95106.22	3.657931	0.184714	0.006949	0.398179
0.15	0.436	24.98095	128931.4	4.958900	0.400135	0.021570	1.235916
0.2	0.436	24.98095	120195.5	4.622907	0.639680	0.047566	2.725343
0.25	0.436	24.98095	110481.4	4.249287	0.861485	0.085095	4.875606
0.3	0.436	24.98095	101486.7	3.903337	1.065301	0.133265	7.635526
0.35	0.436	24.98095	93221.57	3.585445	1.252520	0.191210	10.95556
0.4	0.436	24.98095	85629.38	3.293437	1.424493	0.258135	14.79010
0.45	0.436	24.98095	78655.52	3.025212	1.582459	0.333309	19.09724
0.5	0.436	24.98095	72249.62	2.778831	1.727560	0.416060	23.83849
0.55	0.436	24.98095	66365.43	2.552516	1.860844	0.505770	28.97850
0.6	0.436	24.98095	60960.47	2.344633	1.983272	0.601873	34.48480
0.65	0.436	24.98095	55995.69	2.153680	2.095730	0.703848	40.32754
0.7	0.436	24.98095	51435.27	1.978279	2.199029	0.811217	46.47933
0.75	0.436	24.98095	47246.25	1.817163	2.293915	0.923541	52.91500
0.8	0.436	24.98095	43398.40	1.669169	2.381074	1.040415	59.61143
0.85	0.436	24.98095	39863.93	1.533228	2.461134	1.161471	66.54738
0.9	0.436	24.98095	36617.31	1.408358	2.534673	1.286366	73.70335
0.95	0.436	24.98095	33635.11	1.293658	2.602224	1.414788	81.06141
1	0.436	24.98095	30895.78	1.188299	2.664273	1.546451	88.60512
1.05	0.436	24.98095	28379.55	1.091521	2.721268	1.681089	96.31934
1.1	0.436	24.98095	26068.25	1.002625	2.773622	1.818461	104.1901
1.15	0.436	24.98095	23945.19	0.920968	2.821712	1.958345	112.2049
1.2	0.436	24.98095	21995.03	0.845962	2.865885	2.100535	120.3518
1.25	0.436	24.98095	20203.70	0.777065	2.906461	2.244843	128.6200
1.3	0.436	24.98095	18558.26	0.713779	2.943732	2.391098	136.9998
1.35	0.436	24.98095	17046.83	0.655647	2.977967	2.539141	145.4820
1.4	0.436	24.98095	15658.50	0.602250	3.009415	2.688825	154.0583
1.45	0.436	24.98095	14383.23	0.553201	3.038301	2.840018	162.7210
1.5	0.436	24.98095	13211.82	0.508147	3.064835	2.992597	171.4631
1.55	0.436	24.98095	12135.82	0.466762	3.089208	3.146448	180.2782

```

*****
Roll Pullout
*****
Input:  I-x (slug ft^2)           23168
        I-y (slug ft^2)           123936
        I-z (slug ft^2)           143239
        Reference Area (ft^2)      400
        Reference Span (ft)        34.72
        Density (slug/ft^3)        0.002376
        Speed (ft/s)               400
        Velocity Axis Roll Rate (deg/sec) 180
        Normal Load Factor (g's)    2
        Angle of Attack (deg)       45
        C-n-delta-R (/rad)         -0.08

Output: Dynamic Pressure (lbf/ft^2) 190.08
        Max. Yaw Coefficient due to Roll Pullout -0.02047
        Rudder Deflection to Counter (deg) -14.6666

```


A3. Program FLTCOND

Program FLTCOND was written in Microsoft FORTRAN for IBM compatible PCs. Sample input (with Lotus-123 spreadsheet) and output is shown in Figures 3 & 4 respectively. Note the value column in the input worksheet is to be written to a file FCINPUT.PRN to be read by FLTCOND. In the output of FLTCOND, variables with values of '.900E+16' signifies that the variable need not be specified in the control power requirement check worksheet discussed in A2.

A4. Programs TRIM1 & TRIM2

Based on "A Closed-form Trim Solution Yielding Minimum Trim Drag for Airplanes with Multiple Longitudinal Control Effectors" by K. H. Goodrich, et al. (NASA TP-2907, May 1989), two FORTRAN programs were written to find the optimal (minimum trim drag) trim schedule in 1-g, level-flight for airplanes with three lifting surfaces (TRIM1) or two lifting surfaces plus thrust vectoring (TRIM2).

DOCUMENTAION FOR 'TRIM1'

Code Written and Documentation Prepared by Jacob Kay
Virginia Tech
September, 1991

1. Objective

This document is to discuss the application and limitations of the program 'TRIM1.'

2. General information

Some recently proposed aircraft configurations use three lifting surfaces. This results in redundant ways of generating moments and forces. Consequently, there are many approaches to trim such airplanes. 'TRIM1' is based on NASA TP-2907, which utilizes the linear optimum trim solution (LOTS), derived using a Lagrange formulation. It determines the longitudinal lift distribution (between the three surfaces) resulting in minimum trim drag in level, steady state flight. In addition, the program also provides the deflection angles for the surfaces to generate the desired lift distribution.

3. Input

Airplane geometry and pertinent parameters to the LOTS are listed in the ASCII file '3SURFACE.DAT', which is included here as the sample input file. Users must be careful to follow the units prescribe for each parameter and not to change the format of the values on the right column. Some input variables require additional discussion, and they are listed below.

- a. l^{cg} (No. 2) is the distance between CG and wing AC normalized with the mean chord of the wing. NOTE: for measurements taken with respect to wing's AC, it is "+" if measured from below and/or behind the wing's AC, and it's "-" if measured from above and/or in front of the wing's AC.
- b. σ/e_{ij} (No.12-17) is the ratio of the Prandtl coefficient and efficiency factor between surface-i and surface-j. They can be obtained by using the apporximation in Appendix C of NASA TP-2907 or by vortex-lattice method (VLM).
- c. δ_f (No. 28) is the optimal wing flap deflection angle (in terms of drag).
Typicall value is zero.

- d. $c-e/c-t$ (No. 35) is the ratio of the elevator chord to the H. tail chord. If all-moving (variable incident) tail is used, enter zero for this value. The program will determine the proper incident angle.
- e. $c-cf/c-c$ (No. 38) is the ratio of the canard's flap chord to the canard chord. Enter zero if all-moving (variable incident) canard is used.

4. Output

There are six parameters that are generated as the final outputs of the program. $CL(1)$, $CL(2)$ and $CL(3)$ represent the lift coefficients of wing, horizontal tail and canard respectively. The last three angles are the fuselage inclination angle (AOA), the horizontal tail deflection angle and the canard deflection angle, respectively. After executing 'TRIM1,' these values can be found on the screen and in the ASCII file 'RESULTS.'

Sample input data for the three surface code TRIM1

1.	Total lift coeff.	(W-bar)	+1.600E-00
2.	Zero-lift Moment Coeff.	(C-m, 0)	-1.000E-01
3.	C.G. distance from wing AC	(l^-cg)	-1.500E-01
4.	Area of Wing, ft ²	(S-1)	+1.670E+02
5.	Area of H. tail, ft ²	(S-2)	+4.140E+01
6.	Area of Canard, ft ²	(S-3)	+2.230E+01
7.	Span of Wing, ft	(b-1)	+4.650E+01
8.	Span of H. tail, ft	(b-2)	+1.370E+01
9.	Span of Canard, ft	(b-3)	+1.060E+01
10.	Wing AC to H. tail AC, ft	(l-2)	+1.551E+01
11.	Wing AC to Canard AC, ft	(l-3)	-2.155E+01
12.	Influence coeff-wing	(sigma/e-11)	+1.000E+00
13.	Influence coeff-H tail	(sigma/e-22)	+1.000E+00
14.	Influence coeff-canard	(sigma/e-33)	+1.000E+00
15.	Influence coeff-wing-tail	(sigma/e-12)	+2.030E-01
16.	Influence coeff-wing-canard	(sigma/e-13)	+1.900E-01
17.	Influence coeff-tail-canard	(sigma/e-23)	+1.440E-01
18.	Wing Mean chord length, ft	(c-bar)	+3.591E+00
19.	Free stream Mach number	(M-infinity)	+5.000E-01
20.	Wing max thickness swp, rad	(lambda-t/c-1)	+0.000E+00
21.	Tail max thickness swp, rad	(lambda-t/c-2)	+4.363E-01
22.	Canard max thick. swp, rad	(lambda-t/c-3)	+0.000E+00
23.	Wing chord/4 sweep, rad	(lambda-c/4-1)	+0.000E+00

24.	H tail chord/4 swp, rad	(lambda-c/4-2)	+4.363E-01
25.	Canard chord/4 swp, rad	(lambda-c/4-3)	+0.000E+00
26.	Flap chord/total wing chord	(c-f/c-w)	+2.000E-01
27.	Wing thickness ratio	(t/c-1)	+1.000E-01
28.	Optimal flap deflection,rad	(delta-f)	+1.745E-02
29.	Incident angle of wing,rad	(i-wing)	+3.491E-02
30.	Taper ratio of wing	(TR-1)	+7.500E-01
31.	Taper ratio of H tail	(TR-2)	+8.200E-01
32.	Taper ratio of canard	(TR-3)	+9.000E-01
33.	H. Tail Height, ft	(h-2)	+6.464E+00
34.	Canard height, ft	(h-3)	-2.227E+00
35.	Elevator-tail chord ratio	(c-e/c-t)	+0.000E-00
36.	H tail tickness ratio	(t/c-2)	+1.200E-01
37.	H tail incident angle, rad	(i-tail)	+0.000E-00
38.	Canard flap-chord ratio	(c-cf/c-c)	+0.000E-00
39.	Canard thickness ratio	(t/c-3)	+8.000E-02
40.	Canard incident angle, rad	(i-canard)	+0.000E-00

Sample ouput from trim1 :

CL-WING	CL-H. TAIL	CL-CANARD	AOA	DELTA-TAIL	DELTA-CANARD
1.5553	-0.0280	0.3869	12.1841	-12.5936	-4.6823
DEFLECTION ANGLE (DEG) = -9.558					

DOCUMENTATION FOR PROGRAM 'TRIM2'

Prepared by Jacob Kay
Virginia Tech
October, 1991

1. Objective

This document is to discuss the application and limitations of the program 'TRIM2.'

2. General information

Some of the recently proposed aircraft configurations call for two lifting surfaces plus thrust vectoring which result in the redundant ways of generating moments and forces. Consequently there are many approaches to trim such airplanes. 'TRIM2' is based on NASA TP-2907 which utilizes the linear optimum trim solution (LOTS), derived using a Lagrange formulation. It determines the longitudinal lift distribution (between the two surfaces and the jet nozzle deflection angle) to result in minimum trim drag in level, steady state flight. In addition, the program also provide the deflection angles for the two lifting surfaces to generate the desired lift distribution.

3. Input

Airplane geometry and pertinent parameters to the LOTS are listed in the ASCII file '2SURFACE.DAT.' Because of the constraints by 'TRIM2,' users must be careful to follow the units prescribe for each parameter and not to change the format of the values on the right column. Some input variables require additional discussion, and they are listed

below. This program can also be applied to airplanes with canard configuration by entering the canard geometry in place of the horizontal tail geometry.

- a. l^{cg} (No. 3) is the distance between CG and wing AC normalized with the mean chord of wing.
NOTE: for measurements taken with respect to wing's AC, it is "+" if measured from below and/or behind the wing's AC, and it's "-" if measured from above and/or in front of the wing's AC.
- b. σ/e_{ij} (No. 10-12) is the ratio of the Prandtl coefficient and efficiency factor between surface-i and surface-j. They can be obtained by using the approximation in Appendix C of NASA TP-2907 or by vortex-lattice method (VLM).
- c. k_1 & k_2 (No. 13 & 14) are the induced lift parameter of wing and horizontal tail due to thrust vectoring. The induced lift coefficient (due to thrust vectoring) is equal to the product of k , deflection angle and thrust coefficient. k is a constant depending on surface and nozzle factors. No analytical approach to determine the value of k is known to the authors of NASA TP-2907 at the time of publication. However, in general, the value of k approaches zero if there exists significant separation between the jet nozzle and the surface.
- d. μ_{TL} (No. 15) is the fraction of thrust loss due to thrust vectoring. It is equal to 1 minus the fraction of thrust recovery. Thrust recovery takes the form of reduced induced drag as the consequence of the upwash field created in front of the surfaces of the airplane by the directed jet. μ_{TL} generally have a value between 0.0 and 0.5.
- e. C_T (No. 16) is the thrust coefficient which is obtained by dividing thrust by the product of dynamic pressure and reference area. C_T is about equal to the total drag

coefficient provided the jet nozzle deflection angle is relatively small.

- f. $\delta-f$ (No. 26) is the optimal wing flap deflection angle (in terms of drag). The typical value is zero.
- g. $c-e/c-t$ (No. 35) is the ratio of the elevator chord to the H. tail chord. If all-moving (variable incident) tail is used, enter zero for this value. The program will determine the proper incident angle.

4. Output

There are five parameters generated as the final outputs of the program. $CL(1)$ and $CL(2)$ represent the lift coefficients of wing and horizontal tail (or canard). The fuselage inclination angle (AOA), the horizontal tail (or canard) deflection angle and the jet nozzle deflection angle are included. Note that the jet nozzle deflection angle is measured with respect to the fuselage reference line. It is "+" if pointing down and "-" if pointing up. Because of the uncertainty involved in the estimation of thrust coefficient and the supercirculation parameters such as k_1 , k_2 and $\mu-TL$, the results generated may require experimental validation. After executing 'TRIM2,' these values can be found on the screen and in the ASCII file 'RESULTS.'

Sample case for thrust vectoring code, TRIM2

1.	Total lift coeff.	(W-bar)	+2.000E-01
2.	Zero-lift Moment Coeff.	(C-m,0)	-1.000E-01
3.	C.G. distance from wing AC	(l^-cg)	-5.600E-02
4.	Area of Wing, ft^2	(S-1)	+4.000E+02
5.	Area of H. tail, ft^2	(S-2)	+8.810E+01
6.	Span of Wing, ft	(b-1)	+3.750E+01
7.	Span of H. tail, ft	(b-2)	+1.470E+01
8.	Wing AC to H. tail AC, ft	(l-2)	+1.493E+01
9.	Wing AC to jet nozzle, ft	(l-3)	+1.920E+01
10.	Influence coeff-wing	(sigma/e-11)	+1.000E+00
11.	Influence coeff-H tail	(sigma/e-22)	+1.000E+00
12.	Influence coeff-wing-tail	(sigma/e-12)	+1.160E-01
13.	Induced lift parameter W-THR(k1)		+0.000E+00
14.	Induced lift parameter T-THR(k2)		+0.000E+00
15.	Fraction of thrust-loss	(MU-TL)	+5.000E-01
16.	Thrust coefficient	(C-T)	+2.000E-01
17.	Free stream Mach number	(M-infinity)	+5.000E-01
18.	Wing max thickness swp, rad	(lambda-t/c-1)	+3.491E-01
19.	Tail max thickness swp, rad	(lambda-t/c-2)	+6.981E-01
20.	Wing incident angle, rad	(i-1)	+0.000E-00
21.	Exhaust Nozzle height, ft	(z-3)	+0.000E+00
22.	Wing chord/4 sweep, rad	(lambda-c/4-1)	+3.491E-01
23.	H tail chord/4 swp, rad	(lambda-c/4-2)	+6.981E-01
24.	Flap chord/total wing chord	(c-f/c-w)	+2.000E-01
25.	Wing thickness ratio	(t/c-1)	+8.000E-02
26.	Optimal flap deflection,rad	(delta-f)	+0.000E-00
28.	Taper ratio of wing	(TR-1)	+3.500E-01
29.	Taper ratio of H tail	(TR-2)	+4.600E-01
30.	H. Tail Height, ft	(h-2)	+5.335E-01
35.	Elevator-tail chord ratio	(c-e/c-t)	+0.000E-00
36.	H tail tickness ratio	(t/c-2)	+6.200E-02
37.	H tail incident angle, rad	(i-tail)	+9.999E-00

Sample output from trim2:

WING C-L = 0.2584

TAIL OR CANARD C-L = -0.2103

JET DEFLECTION ANGLE (DEG) = -7.381

FUSELAGE ANGLE OF ATTACK (DEG) = 4.510

CANARD/TAIL DEFLECTION ANGLE (DEG) = -9.558

Appendix B. Literature Search:

Control Power Requirements

Primary Papers

Mangold, P. "Integration of Handling Quality Aspects into the Aerodynamic Design of Modern Unstable Fighters." *Flying Qualities*, AGARD-CP-508.

Issues relating instabilities in longitudinal and lateral-directional controls to flying qualities are discussed.

Chody, J.; Hodgkinson, J. and Skow, A. "Combat Aircraft Control Requirements for Agility." *Aerodynamics of Combat Aircraft Control and of Ground Effects*. AGARD CP-465, Oct. 1989. Section 2.0 - 3.3.

Additional lateral-directional stability criteria are introduced to augment the traditional Weissman Criteria in the preliminary design process.

Renzo, B. "Flying Qualities Experience on the AMX Aircraft." *Flying Qualities*. AGARD-CP-508.

The application of modern handling qualities criteria to the AMX lead to the alleviation of PIO tendencies and accomplishing lateral-directional precision tracking tasks.

Innocenti, M. "Metrics for Roll Response Flying Qualities." *Flying Qualities*. AGARD-CP-508.

The primary focus is the analysis using the Gibson's method and composed of time domain and frequency domain techniques to evaluate the roll performance and handling qualities of a highly augmented aircraft.

Mercadante, R. "Basic Agility/Control Power Requirements for Advanced Supersonic Fighter Configuration." Grumman Memorandum, No. EG-ARDYN-83-82. Oct 27, 1983.

A simplified analysis leading to the rapid estimation of configuration control power to satisfy agility requirements is presented.

Saunders, T and Tucker, J. "Combat Aircraft Control Requirements." *Aerodynamics of Combat Aircraft Controls and of Ground Effects*. AGARD CP-465, Oct. 1989.

A qualitative discussion of functions and requirements of controls with examples from existing British fighter/attack aircraft.

Gibson, J. "The Development of Alternate Criteria for FBW Handling Qualities." *Flying Qualities*. AGARD-508.

This paper presents the development of criteria to address problems in flight path, flight attitude, PIO, and Lateral-directional handling.

Buchacker, E.; Galleithner, H.; Koehler, R. and Marchand, M. "Development of MIL-8785C into a Handling Qualities Specification for a New European Fighter Aircraft." *Flying Qualities*. AGARD-508.

This paper focused on the introduction of additional criteria (such as higher order system criteria, carefree handling) and the amendments of application of pertinent criteria of MIL-8785C to the development of Handling Qualities Definition Documents (HQDD) for the EFA.

Wunnenberg, Horst. "Handling Qualities of Highly Augmented Unstable Aircraft, Summary of an AGARD-FMP Working Group Effort." *Handling Qualities*. AGARD CP-508.

This is a very brief outline of AGARD AR-279 that

presents methods and criteria as design guides and for the evaluation of handling qualities of highly augmented aircraft.

Moorhouse, D.; Citurs, K.; Thomas, R. and Crawford, M. "The Handling Qualities of the STOL & Maneuver Technology Demonstrator from Specification to Flight Test." *Handling Qualities*. AGARD CP-508.

This paper presents the analytical development of the handling qualities specifications of the S/MTD aircraft. Simulator verification and flight test results are also included.

Secondary Papers:

Advisory Group for Aerospace Research & Development. "Manoeuvre Limitations of Combat Aircraft." AGARD-AR-155A.

The descriptions of various phenomena limiting aircraft maneuverability, and the approaches to determine the manoeuver limits are presented.

Fellers, W.; Bowman, W. and Wooler, P. "Tail Configuration for Highly Maneuverable Combat Aircraft." *Combat Aircraft Maneuverability*. AGARD CP-517, Oct. 1989.

A comparison in maneuverability for three tail configurations, aft tail, tailless (with and without thrust vectoring) and canard configuration is presented.

Thomas, D. "The Art of Flying Qualities Testing." *Flying Qualities*. AGARD CP-508.

From a test pilot's point of view, the author argues for less of the unnecessary numbers and regulations in MIL-specs & FAR. He uses examples to illustrate that an airplane with good flying qualities is one that performs well in actual flight no just on paper.

Leggett, D. and Black, G. "MIL-STD-1797 is not a Cookbook." *Flying Qualities*. AGARD CP-508.

The authors claim that the subjective, closed-loop requirements of the MIL-STD-1797 come closer to specifying qualities than do the objective, open-loop requirements. They further believe that MIL-STD-1797 should be used as a specification (rather than a guideline), but designers should keep in mind that it's more important to meet the specifications' intents than just the specifications' criteria.

Sobata, M. "B-1B High AOA Testing in the Evaluation of a Stall Inhibitor System." *Flying Qualities*. AGARD CP-508.

This paper summarizes the application of Stall Inhibitor System/Stability Enhancement Function (SIS/SEF) to address the longitudinal instability problem of the B-1B.

Walchli, L. and Smith, R. "Flying Qualities of the X-29 Forward Swept Wing Aircraft." *Flying Qualities*. AGARD CP-508.

A brief description of the flight control system and a summary of the subsequent high and low AOA flight test results of the flying qualities are presented.

Mazza, C. "Agility: A Rational Development of Fundamental Metrics and Their Relationship to Flying Qualities." *Flying Qualities*. AGARD CP-508.

The Frenet approach and the Newtonian approach for the assessment of aircraft agility are discussed.

McKay, K. and Walker, M. "A Review of High Angle of Attack Requirements for Combat Aircraft." *Flying Qualities*. AGARD CP-508.

The paper examines qualitatively the implications of

designing for high angle of attack on aircraft design configuration.

Herbst, W. "X-31 at First Flight." *Flying Qualities*. AGARD CP-508.

The motivation and design goals are discussed along with the expected performance in terms of "supermaneuverability."

Wanner, J. and Carlson, J. "Comparison of French and United States Flying Qualities Requirements." *Handling Qualities Criteria*. AGARD CP-106.

The goals and intent of the two sets of flying qualities requirements are shown to be generally the same.

Andrews, S. "The Nature and Use of the Rules for Judging the Acceptability of the Flying Qualities of Fixed Wing Aircraft." *Handling Qualities Criteria*. AGARD CP-106.

This paper considers the general content of "Design Requirements for Service Airplane" and "Flying Qualities of Piloted Aeroplane" in relation to the requirements of the flight test in the assessment of fighter/attack aircraft.

Sliff, R. and LeSuer, R. "FAA Flying Qualities Requirements." AGARD CP-106.

Projected difficulties associated with airplane handling qualities indicates a need for flexibility and change of FAR to accommodate new designs and innovations.

Anderson, S. and Schroers, L. "Revisions to V/STOL Handling Qualities Criteria of AGARD Report 408." AGARD CP-106.

Several controversial areas associated with V/STOL aircraft are discussed to show that more research is

needed to refine their criteria.

Doetsch, K. Jr. "Parameters Affecting Lateral-Directional Handling Qualities at Low Speed." AGARD CP-106.

Some additional parameters of V/STOL aircraft are found to affect the lateral-directional flying qualities at very low speeds.

ADDITIONAL REFERENCES:

Gibson, J. "Piloted Handling Qualities Design Criteria for High Order Flight Control System" AGARD CP-333, April 1982.

Hodgkinson, J. and LaManna, W. "Equivalent System Approaches to Handling Qualities Analysis and Design Problems of Augmented Aircraft" AIAA Atmospheric Flight Conference, Hollywood, FL, August 1977.

Gallagher, J. and Nelson, W. Jr. "Flying Qualities of the Northrop YF-17 Fighter Prototypes" Business Aircraft Meeting, Wichita. March 1977.

Skow, A. and Titiriga, A. Jr. "A Survey of Analytical and Experimental Techniques to Predict Aircraft Dynamic Characteristics at High Angle of Attack." AGARD-CP-235, May 1978.

Gibson, J. "Handling Qualities for Unstable Combat Aircraft", ICAS-86-5.3.4, September 1986.

Gibson, J. "Evaluation of Alternate Handling Qualities Criteria for Highly Augmented Unstable Aircraft", AIAA Paper 90-2844.

Bland, M. et al. "Alternative Design Guidelines for Pitch Tracking", AIAA 87-2289, August 1987.

Hoh, R. "Concepts and Criteria for a Mission Oriented Flying Qualities Specification", AGARD LS-157, May 1988.

Moorhouse, D. Laughrey, J. and Thomas, R. "Aerodynamic Propulsive Control Development of the STOL and Maneuver

Technology Demonstrator", AGARD CP-465, October 1989.

Monagan, S. et al. "Lateral Flying Qualities of Highly Augmented Fighter Aircraft", AFWAL-TR-81-3171, Vol I, 1982.

Innocenti, M. and Thukral, A. "Roll Performance Criteria for Highly Augmented Aircraft", AIAA Journal of Guidance Control and Dynamics.

McRuer D. "Progress and Pitfalls in Advanced Flight Control Systems", AGARD-CP-321.

Beaufreere, H. "Flight Plan Development for a Joint NASA/Navy High Angle of Attack Flight Test Program", Grumman Contract Nol. NASA 2965, March 1983.

Greer, H. "Summary of Directional Divergence Characteristics of Several High Performance Aircraft Configurations", NASA-TN D-6993, Nov. 1972.

Mangold, P. and Wedekind G. "'Inflight Thrust Vectoring' a Further Degree of Freedom in the Aerodynamic/Flightmechanical Design of Modern Fighter Aircraft", AGARD CP-465, Madrid 1989.

Bosworth, J. and Cox, H. "A Design Procedure for the Handling Qualities Optimization of the X-29A Aircraft," AIAA 89-3428, Boston, Mass., August 1989.

Kalviste, J. "Measures of Merit for Aircraft Dynamic Maneuvering", SAE Technical Paper 901005, April 1990.

Brandon, J. and Nguyen, L. "Experimental Study of Effects of Forebody Geometry on High Angle of Attack Static and Dynamic Stability." AIAA 86-0311.

Chambers, J. and Anglin E. "Analysis of Lateral-directional Stability Characteristics of a Twin Jet Fighter Airplane at High Angles of Attack." NASA TN-D-5361.

Maul, M. and Paulson, J. "Dynamic Lateral Behavior of High Performance Aircraft." NASA RML58E16.

Pinsker, W. "Directional Stability in Flight with Bank Angle Constraint as a Condition Defining a Minimum Acceptable Value for n-v." RAE Report TR 67127.

Weissman, R. "Criteria for Predicting Spin Susceptibility of Fighter Type Aircraft." AST TR 72-48.

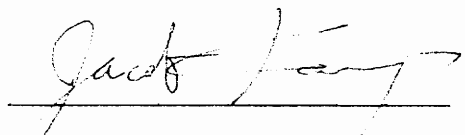
Kalviste, J. "Aircraft Stability Characteristics at High Angle of Attack." AGARD CP-235 Paper 29.

Carr, P. and Gilbert, W. "Effects of Fuselage Forebody Geometry on the Low Speed Lateral Directional Characteristics of Twin-tail Fighter Model at High Angles of Attack." NASA TP-1592.

Skow, A. "Forebody Vortex Blowing - A Novel Control Concept to Enhance Departure/ Spin Recovery Characteristics of Fighter & Trainer Aircraft." AGARD CP-262, Paper 24.

Vita

The author was born in Taiwan on July 11, 1968. He and his family moved to Hawaii in 1982 and later became residents of Southern California in 1985. Under the unconditional support of his parents, the author showed interest in science and mathematics. In 1987, he graduated from San Marino High School where he excelled in chemistry and physics. Later that year, he enrolled in the Aerospace Engineering Program at California State Polytechnic University, Pomona. During his summer internship in 1990, he worked as a lab assistant in the Optical Computation Laboratory at the Jet Propulsion Laboratory. In June of 1991, he graduated with Honors in Aerospace Engineering with a 3.80 GPA. He then proceeded to work on his Master's degree in Aerospace Engineering later that year at Virginia Tech under the supervision of Dr. W. H. Mason. During the summer of 1992, he worked as an intern at NASA Langley Research Center to study the stratospheric ozone depletion problem and explore the feasibility of vehicle-based countermeasure schemes. Upon graduation, the author wishes to continue working in the areas of aircraft design and flight dynamics.



Jacob Kay